CONVOLUTIONAL NEURAL NETWORK LEARNING APPROACHES FOR DRIVER INJURY SEVERITY CLASSIFICATION AND APPLICATION IN SINGLE-VEHICLE CRASHES IN RITI COMMUNITIES

FINAL PROJECT REPORT

by

Guohui Zhang, Ph.D., Hanyi Yang, Ph.D., Hao Yu, Ph.D., and Runze Yuan, Ph.D.

Department of Civil and Environmental Engineering
University of Hawaii at Manoa

for

rural · isolated · tribal · indigenous

DISCLAIMER

The contents of this report reflect the views of the authors, who are responsible for the facts and the accuracy of the information presented herein. This document is disseminated under the sponsorship of the U.S. Department of Transportation's University Transportation Centers Program, in the interest of information exchange. The Center for Safety Equity in Transportation, the U.S. Government and matching sponsor assume no liability for the contents or use thereof.

TECHNICAL REPORT DOCUMENTATION PAGE

1. Report No.	2. Government Accession No.	3. Recipient's Catalog No.

4. Title and Subtitle	5. Report Date
Convolutional Neural Network Learning Approaches for Driver Injury Severity Classification and Application in Single-Vehicle Crashes in RITI Communities	June 30, 2024
	6. Performing Organization Code

7. Author(s) and Affiliations	8. Performing Organization Report No.
Guohui Zhang, Ph.D., P.E., Hanyi Yang, Ph.D., Hao Yu, Ph.D., and Runze Yuan, Ph.D. Department of Civil and Environmental Engineering University of Hawaii at Manoa	INE/CSET 24.07

9. Performing Organization Name and Address	10. Work Unit No. (TRAIS)
Center for Safety Equity in Transportation ELIF Building Room 240, 1760 Tanana Drive Fairbanks, AK 99775-5910	
	11. Contract or Grant No.

12. Sponsoring Organization Name and Address	13. Type of Report and Period Covered
United States Department of Transportation Research and Innovative Technology Administration 1200 New Jersey Avenue, SE Washington, DC 20590	Research Report
	14. Sponsoring Agency Code

15. Supplementary Notes

Report uploaded to:

16. Abstract

It is crucial to examine the characteristics and attributes of traffic crashes in Rural, Isolated, Tribal, or Indigenous (RITI) communities using statistical and data-driven methods. However, traditional crash data analysis faces challenges due to unobserved heterogeneities and temporal instability. To address these issues, a fusion convolutional neural network with random term (FCNN-R) model is developed for driver injury severity analysis. The proposed model consists of a set of sub-neural networks (sub-NNs) and a multi-layer convolutional neural network (CNN). Seven-year (2010-2016) single-vehicle crash data is applied. The proposed model outperformed other five typical approaches in the predictability comparison. In addition, unobserved heterogeneity, which has been recognized as a critical issue in crash frequency modelling, generates from multiple sources, including observable and unobservable factors, space and time instability, crash severities, etc. In this project, hierarchical Bayesian random parameters models with various spatiotemporal interactions are further developed to address as well. Selected for analysis are the yearly county-level alcohol/drug impaired-driving related crash counts data of three different injury severities including minor injury, major injury, and fatal injury in Idaho from 2010 to 2015. Significant temporal and spatial heterogenous effects are detected in all three crash severities. These empirical results support the incorporation of temporal and spatial heterogeneity in random parameters models.

17. Key Words	18. Distribution Statement
Traffic safety, Fatality pattern, injury severity, Deep neural network	

19. Security Classification (of this report)	20. Security Classification (of this page)	21. No. of Pages	22. Price
Unclassified.	Unclassified.		N/A

Form DOT F 1700.7 (8-72) **Reproduction of completed page authorized.**

SI* (MODERN METRIC) CONVERSION FACTORS

APPROXIMATE CONVERSIONS TO SI UNITS

Symbol	When You Know	Multiply By	To Find	Symbol
		LENGTH		
in	inches	25.4	millimeters	mm
ft	feet	0.305	meters	m
yd	yards	0.914	meters	m
mi	miles	1.61	kilometers	km
		AREA		
in^2	square inches	645.2	square millimeters	mm^2
ft^2	square feet	0.093	square meters	m^2
yd^2	square yard	0.836	square meters	m^2
ac	acres	0.405	hectares	ha
mi^2	square miles	2.59	square kilometers	km^2
		VOLUME		
fl oz	fluid ounces	29.57	milliliters	mL
gal	gallons	3.785	liters	L
ft^3	cubic feet	0.028	cubic meters	m^3
yd^3	cubic yards	0.765	cubic meters	m^3
		NOTE: volumes greater than 1000 L shall be shown in m^3		
		MASS		
oz	ounces	28.35	grams	g
lb	pounds	0.454	kilograms	kg
T	short tons (2000 lb)	0.907	megagrams (or "metric ton")	Mg (or "t")
		TEMPERATURE (exact degrees)		
^oF	Fahrenheit	5 (F-32)/9 or (F-32)/1.8	Celsius	^oC
		ILLUMINATION		
fc	foot-candles	10.76	lux	lx
fl	foot-Lamberts	3.426	candela/m^2	cd/m^2
		FORCE and PRESSURE or STRESS		
lbf	poundforce	4.45	newtons	N
lbf/in^2	poundforce per square inch	6.89	kilopascals	kPa

APPROXIMATE CONVERSIONS FROM SI UNITS

Symbol	When You Know	Multiply By	To Find	Symbol
		LENGTH		
mm	millimeters	0.039	inches	in
m	meters	3.28	feet	ft
m	meters	1.09	yards	yd
km	kilometers	0.621	miles	mi
		AREA		
mm^2	square millimeters	0.0016	square inches	in^2
m^2	square meters	10.764	square feet	ft^2
m^2	square meters	1.195	square yards	yd^2
ha	hectares	2.47	acres	ac
km^2	square kilometers	0.386	square miles	mi^2
		VOLUME		
mL	milliliters	0.034	fluid ounces	fl oz
L	liters	0.264	gallons	gal
m^3	cubic meters	35.314	cubic feet	ft^3
m^3	cubic meters	1.307	cubic yards	yd^3
		MASS		
g	grams	0.035	ounces	oz
kg	kilograms	2.202	pounds	lb
Mg (or "t")	megagrams (or "metric ton")	1.103	short tons (2000 lb)	T
		TEMPERATURE (exact degrees)		
^oC	Celsius	1.8C+32	Fahrenheit	^oF
		ILLUMINATION		
lx	lux	0.0929	foot-candles	fc
cd/m^2	candela/m^2	0.2919	foot-Lamberts	fl
		FORCE and PRESSURE or STRESS		
N	newtons	0.225	poundforce	lbf
kPa	kilopascals	0.145	poundforce per square inch	lbf/in^2

*SI is the symbol for the International System of Units. Appropriate rounding should be made to comply with Section 4 of ASTM E380.
(Revised March 2003)

TABLE OF CONTENTS

LIST OF FIGURES

LIST OF TABLES

EXECUTIVE SUMMARY

This report documents the research activities undertaken to investigate machine learning approaches to formulate traffic crashes in Rural, Isolated, Tribal, or Indigenous (RITI) communities that result in significant incapacitating injuries and losses. Traffic crashes in these communities are often associated with factors such as speeding, low utilization of safety devices (e.g., seat belts), adverse climate and weather conditions, poor road maintenance and repairs, and inadequate lighting conditions, which differ from those in urban areas. Therefore, it is crucial to examine the characteristics and attributes of traffic crashes in RITI areas using statistical and data-driven methods. However, traditional crash data analysis faces challenges due to unobserved heterogeneities and temporal instability.

To address these issues, a fusion convolutional neural network with random term (FCNN-R) model is developed for driver injury severity analysis. The proposed model consists of a set of sub-neural networks (sub-NNs) and a multi-layer convolutional neural network (CNN). More specifically, the sub-NN structure is designed to deal with categorical variables in crash records; multi-layer CNN structure captures the potential nonlinear relationship between impact factors and driver injury severity outcomes. Seven-year (2010-2016) single-vehicle crash data is applied. Models with different CNN layers are tested using the validation set, as well as various model layouts with and without a dropout layer or regularization term in the objective function. It is found that different model layouts provide consistent predictive performance. With the limited training data, more CNN layers result in the prematurity of the training procedure. The dropout layer and the regularization technique help improve the stability of the effects of different variables. The proposed model outperformed other five typical approaches in the predictability comparison. Moreover, a marginal effect analysis was conducted to the proposed FCNN-R model, the FCNN model and the mixed multinomial logit model. It shows that the proposed FCNN-R model can be used to uncover the underlying correlations similar to the traditional statistical models. Additionally, the temporal stability of the proposed FCNN-R approach is discussed based on the model performance in different years. Future research is recommended to include more information for improving the universality of the proposed approach.

In addition, unobserved heterogeneity, which has been recognized as a critical issue in crash frequency modelling, generates from multiple sources, including observable and unobservable factors, space and time instability, crash severities, etc. However, only a very limited body of research is dedicated to distinguish and simultaneously address all these sources of unobserved heterogeneity. In this project, hierarchical Bayesian random parameters models with various spatiotemporal interactions are further developed to address this issue. Selected for analysis are the yearly county-level alcohol/drug impaired-driving related crash counts data of three different injury severities including minor injury, major injury, and fatal injury in Idaho from 2010 to 2015. The variables, including daily vehicle miles traveled (DVMT), the proportion of male (MALE), unemployment rate (UR), and the percentage of drivers of 25 years and older with a bachelor's degree or higher (BD), are found to have significant impacts on crash frequency and be normally distributed in certain crash severities. Significant temporal and spatial heterogenous effects are also detected in all three crash severities. These empirical results support the incorporation of temporal and spatial heterogeneity in random parameters models.

CHAPTER 1. INTRODUCTION

1.1. Problem Statement

Traffic safety is one of the essential areas for transportation researchers due to socioeconomic costs of traffic crashes. It was reported that 33 thousand people lost their lives, 4.5 million people were injured, and 24 million vehicles were damaged in motor vehicle crashes in the United States in 2015 (Blincoe et al., 2015). The economic costs of these crashes totaled $242 billion, accounting for 1.6% percent of US gross domestic product for 2015. Hence, significant efforts have been devoted to developing a better understanding of driver injury severity and the impact factors in the past decades. Additionally, crashes in rural areas lead to significant incapacitating injuries and losses, particularly affecting rural, isolated, tribal, and indigenous (RITI) communities. According to the National Highway Traffic Safety Administration (NHTSA) report by the US Department of Transportation (USDOT), the fatality rate in rural areas is double that of urban areas (Al-Marshad et al., 2013). Furthermore, the Hawaii Department of Transportation (HDOT) (Highway Safety Annual Report, 2014) indicates that the fatality rate in rural areas was 195% higher than in urban areas.

Traffic crashes in RITI communities demonstrate significantly different properties from those in urban areas. More factors such as speeding, low usage of safety devices (e.g., seatbelts), adverse weather conditions, poor maintenance and repair of roads, and inadequate lighting will contribute to the increased severity of crashes in these communities. Therefore, it is crucial to study the properties and attributes of traffic crashes in RITI areas using data analysis methods, including statistical and data-driven approaches. However, the studying crash severity in RITI areas is not enough. This study aims to contribute to the literature and minimizes the shortcomings of prior crash severity prediction models by developing novel deep learning approaches.

To address the research gap, the tasks in this project include: 1) A fusion convolutional neural network with random term (FCNN-R) model is proposed for single-vehicle crash driver injury severity analysis; and 2) The hierarchical Bayesian random parameters models with various spatiotemporal interactions are developed to address the crash frequency problem with unobserved heterogeneity in the state of Idaho from 2010 to 2015.

This research enhances traffic safety program management across all levels in RITI communities by guiding the design and implementation of targeted countermeasures to reduce the severity and risk of rural crashes. It highlights the significant role of weather conditions, indirectly indicating how climate change affects crash outcomes and injury severity. The upgraded crash data platform will introduce more advanced features, while the use of Bayesian approaches and finite mixture random parameter models provides crucial insights into crash data analysis within RITI communities.

The examination of rural crash data will greatly assist in developing proactive strategies to lower crash risks and severities in RITI communities. According to our comprehensive literature review, there is no existing study that explores driver injury severity patterns in low-visibility crashes, taking into account finite mixture random effects and handling missing data. This lack of research inspired us to perform a fundamental methodological analysis of rural crash characteristics in RITI communities.

.

1.2. Research Objectives

This project aimed at developing a variety of deep learning methods to analyze the specific types of traffic crashes, and proposing a novel finite mixture random parameter model for driver injury severity analysis in RITI communities. Towards this goal, the research objectives were as follows:

- Developing a deep learning model consists of a set of sub-neural networks (sub-NNs) and a multi-layer convolutional neural network (CNN) to analyze the driver severity in single-vehicle crashes on state roads based on seven-years of data.
- Developing the hierarchical Bayesian random parameters models with various spatiotemporal interactions are developed to address the crash frequency problem with unobserved heterogeneity.

1.3. Report Organization

Chapter 2 provides an extensive review of prior research pertinent to this study, covering areas such as crash severity prediction problem, and the crash frequency problem. Chapter 3 introduces a deep learning model consists of a set of sub-neural networks (sub-NNs) and a multi-layer convolutional neural network (CNN) to analyze the driver severity in single-vehicle crashes on state roads based on seven-years of data. Chapter 4 concentrates on the hierarchical Bayesian random parameters models with various spatiotemporal interactions are developed to address the crash frequency problem with unobserved heterogeneity. Finally, Chapter 5 presents the conclusion of this research and the recommendations for future research.

CHAPTER 2.   LITERATURE REVIEW

2.1.   Generic Crash Severity Modeling and Analysis

In a traffic crash, the initial point of impact affects the severity, and data shows the probability of fatality increases when the point of impact is front (National Highway Traffic Safety Administration (NHTSA), 2019), but it should also depend on vehicle numbers in a crash and on crash types. It is found that, in a car-following behavior, the size of a vehicle affects the visibility of the following cars, and the vehicle's mass influences the magnitude of the vehicle's sudden acceleration and deceleration (Abdel-Aty and Abdelwahab, 2003; Erbulut, 2014). Vehicles with larger mass, such as vans, pickup trucks, and station wagon cars, tend to have lower severity level in a rear-end crash (Khattak, 2001). However, these large vehicles lead to more severe driver injuries and fatalities in multi-vehicle crashes than their counterparts, as was revealed in a study by Wu et al. (2014). Because of the small mass, motorcyclists are the most vulnerable and have a high probability to be seriously injured (National Highway Traffic Safety Administration (NHTSA), 2019). Many existing works focus on datasets with large trucks or motorcycles included (Chang and Mannering, 1999; Chen and Chen, 2011; Shaheed and Gkritza, 2014; Shaheed et al., 2013). Shao et al. (2020) applied the random parameters ordered probit model to the rear-end crashes between passenger cars and trucks and found that the crash configurations, which are included as risk factors, are key impact factors. Prajongkha et al. (2023) used ordinal logistic analysis to analyze risk factors in motorcycle rear-end crashes by constructing models for different crash configurations and their results shows that the models are quite different for each crash configuration. Passenger cars and light trucks also vary in vehicle volume, mass, seat height, driver's vision etc., but their differences are comparably smaller compared to those between motorcycle and car or truck and car. How much heterogeneity is induced by these two types of vehicles and other risk factors and how the crash configuration affects the crash severity are of interest to explore. As the two major types of vehicles on the road, few conclusions on their factors impacting severity, together with the high-risk patterns were drawn. Given the large numbers of injuries in passenger cars and light trucks, for injury prevention, it is important to know what are the risk factors for serious injury and how large a difference exists in influencing the crash severity by the two types of vehicles in a rear-end crash. Therefore, in this study, the crash configurations are considered as potential risk factors and the latent class MNL model is used to examine the heterogeneity.

It has been found in contemporary studies that when the number of vehicles in a crash change, the set of impact factors to crash severity also becomes quite different (Chen and Chen, 2011; Dong et al., 2018; Geedipally and Lord, 2010; Ivan et al., 1999; Wu et al., 2014; Yu and Abdel-Aty, 2013a). For a rear-end collision, the driver in the leading vehicle is found to be more severely injured than the driver in the following vehicle in two-vehicle crashes, whereas the driver in the middle car is more severely injured in three-vehicle crashes (Khattak, 2001; Yasmin et al., 2014). Chen et al. (2015) discovered that truck-involvement, and the number of vehicles involved could significantly increase driver injury severities in rear-end crashes. In a rear-end crashes between two passenger cars, driver age, gender, vehicle, airbag or seat belt use, and traffic flow are found to affect injury (Chen et al., 2019). For rear-end crashes with passenger cars and other light-duty vehicles, it is found that passenger cars usually increase injury severity to their drivers and reduced injury severity to the drivers of the vehicles they collide with (Dabbour et al., 2020). From the biomechanics aspect, it is found that in rear-end crashes, the age group of 60 and older and the group of females have high risk of suffering from serious injury (Hell et al.,

2002). Abdel-Aty and Abdelwahab (2003) estimated crash probability based on four different rear-end configurations among passenger cars and light trucks as either leading or following vehicles, and found that sight distance, driving discomfort, and distraction were contributing factors for different configurations. Wang et al. (2022) built models for the probability of each configuration of car-truck rear-end crashes on expressways. Their results revealed that many differences exist among the configurations, indicating different mechanisms of crash configurations, which can also be expected for rear-end crashes between vehicles of passenger cars and pickup trucks, although they are comparably similar in size and mass compared to large truck and motorcycle crashes. Binary discrete model, such as the binary logit and probit model, has been applied in previous studies (Khattak, 2001; Shibata and Fukuda, 1994). Many variations were proposed to overcome the limitations of traditional binary logit and probit models, such as single injury outcome and unobserved effects of impact factors (Savolainen et al., 2011). For instance, Ouyang et al. (2002) proposed a simultaneous binary logit model to determine the impact of significant factors in the presence of multiple injury outcomes simultaneously. Lee and Abdel-Aty (2008) developed bi-variate probit models accounting for underlying correlation among passengers and crash characteristics. For the multiple discrete outcome models, ordered choice approaches that account for the ordinal nature of driver injury outcomes, i.e., from no injury, to possible injury, to serious injury, and fatality was widely employed in driver injury severity studies (Chen et al., 2016; O'donnell and Connor, 1996; Wang and Abdel-Aty, 2008; Xie et al., 2009; Xiong et al., 2014; Yu, H. et al., 2020b; Yu, R. et al., 2020). Alternatively, a multinomial logit model has also been applied during the past decades, which releases the ordinal constraint (Chen et al., 2015; Islam and Mannering, 2006; Shankar et al., 1996; Wu et al., 2016a; Ye and Lord, 2014). However, multinomial logit models are associated with the constraint of the independence of irrelevant alternatives (IIA) property, which assumes that unobserved factors are independent across individual crashes. To deal with the unobserved heterogeneity, a list of techniques is employed, such as: nested logit models, which hierarchically capture the correlation of unobserved factors among severity levels (Hu and Donnell, 2010; Lee and Mannering, 2002; Wu et al., 2016b; Ye and Lord, 2014); random parameter logit models, which uncover unobserved heterogeneity by allowing parameters varying across observations (Li et al., 2019; Wu et al., 2016b, 2014; Ye and Lord, 2014); ordered logit/probit model with random parameters, which handle the ordered nature of crash injury severity and unobserved heterogeneities simultaneously (Fountas et al., 2018; Li et al., 2018; Yu, M. et al., 2020; Zeng et al., 2019, 2020); and latent class models, which address the unobserved heterogeneity by classifying crash data into homogeneous groups (Li et al., 2019, 2018; Xie et al., 2012). The detailed literature review can also be referred to in Savolainen et al. (2011), Mannering and Bhat (2014), and Mannering et al. (2016). The crash configurations, together with the vehicle's relative position in a rear-end crash will be shown to play a key role as both risk and cluster factors to indicate the heterogeneity in variable effects. This indicates that the passenger car and light truck rear-end configurations contribute very differently in the rear-end crashes.

In crash severity analysis, traditional regression models, such as multinomial logit (MNL) /probit model and ordered logit/probit model have been widely used (Chen et al., 2016; Chiou et al., 2013; Greene, 2012; Lee and Mannering, 2002; Mannering and Bhat, 2014; McCullagh, 1980; McFadden, 1980; Shankar and Mannering, 1996; Train, 2009; Yamamoto and Shankar, 2004), with other machine-learning models emerging in recent years (Moussa et al., 2022). The ordered probability models have limitations that might rule out the possibility for an explanatory variable to simultaneously increase or decrease the probabilities of the both the extreme severity categories (Mannering and Bhat, 2014), e.g., not ejected

airbag may simultaneously increase the probability of no injury and fatality, but a decrease of mild injury, therefore the MNL model is chosen in this paper. To address the unobservable heterogeneity issue in existing crash data that are extracted from standard crash reports, the mixed MNL and latent class MNL models were developed and popularly utilized (Behnood and Mannering, 2017; Haleem and Gan, 2013; Mannering and Bhat, 2014; Wu et al., 2013; Ye and Lord, 2011; Yu et al., 2020). Mixed MNL model accommodates the unobservable heterogeneity among individuals by allowing the coefficients, as a distribution, varying across individuals (McFadden and Train, 2000; Train, 2009) while the latent class MNL model addresses the unobservable heterogeneity by statistically grouping the individuals up to a finite number of classes and training different MNL models in different classes (Cerwick et al., 2014). For example, Yu et al., (2020) applied a random parameters approach with heterogeneity in means and variances to analyze the injury severity of rear-end crashes at work zones, during which a significant temporal instability was found in crashes across years. Wang et al. (2022) investigated the temporal stability of factors affecting rear-end and non-rear-end crash severities, also using a random parameter approach with heterogeneity in means and variances and confirmed the temporal instability in both types of crashes. They both have their own merit and latent class MNL was found to have strong statistical support and have the virtue of freeing the analyst from possibly strong or unwarranted distributional assumptions about individual heterogeneity (Greene and Hensher, 2003). As examples of using latent class MNL models, Behnood et al. (2014) adopted it to examine the differences in the injury severity levels regarding sober and alcohol-impaired drivers and showed that there were substantial differences across age/gender groups in the absence/presence of alcohol. Shaheed and Gkritza (2014) applied latent class MNL model to investigate the single-vehicle motorcycle crash and addressed unobserved heterogeneity by identifying two distinct crash data classes with homogeneous attributes. Yu et al. (2020) and Li et al. (2019) developed the latent class MNL models allowing heterogeneity within classes considered for severity modelling in single-vehicle crashes. Certain machine-learning models have shown promising performance in predicting rear-end crash severity, but work more like a "black-box". For instance, Moussa et al., (2022) used a deep residual neural networks model with Monte Carlo simulation to investigate the impact of each explanatory factor on rear-end injury severity, and found the model achieved a satisfactory predicting accuracy of 83%. In our work, the latent class MNL model is used to investigate driver injury severity in two-vehicle rear-end crashes between passenger cars and light trucks, which will help to catch the specific crash patterns regarding to severity and their influence on crash severity.

2.2. Deep Learning Models in Traffic Crash Analyses

Some researchers also applied machine learning approaches in traffic crash analysis. Abdelwahaba and Abdel-Aty (2001, 2002) have applied the multi-layer neural network models for vehicle injury severity classification. Li et al. (2008) predicted motor vehicle crashes using support vector machine models. Delen et al. (2006) applied a series of artificial neural networks to capture the possible nonlinear relationships between injury severity levels and crash factors. Chang and Wang (2006) applied a classification and regression tree approach for crash severity analysis. Zeng and his colleagues further provided a series of formulations on an optimized neural network for both crash risk and crash severity prediction (Zeng et al., 2016a, 2016b; Zeng and Huang, 2014). The machine learning models in these formulations, however, applied only one-hidden layer in nature, which is usually termed as shallow feature learning. Though showing better or comparable predictive performance, these superficial

learning approaches mostly depend on the data characteristics used in the training process and may be prone to overfitting data (Lord and Mannering, 2010; Schmidhuber, 2015; Xie et al., 2007).

Recent advances in artificial intelligence provided an opportunity to formulate multi-hidden-layer learning structures, i.e., deep neural network (DNN), which is capable of learning valid representations of data within unstructured data and provides state-of-art performance in many research fields (Bengio and Delalleau, 2011). DNN approaches have been extensively studied in transportation research, such as short-term traffic flow prediction (Bao et al., 2019b; Lv et al., 2014; Ma et al., 2015b, 2015a), traffic demand estimation (Ke et al., 2017; Yu, H. et al., 2020a), and traffic crash forecast (Bao et al., 2019a), with detailed reviews in Nguyen et al. (2018) and Wang et al. (2018). Considering the possible contributions of the DNN approaches, such as easy application, and outstanding prediction accuracy, the application of the DNN approaches in the field of traffic safety analysis is promising. However, limited studies have been conducted to apply DNN approaches in driver injury severity analysis (Sameen and Pradhan, 2017; Sameen et al., 2017; Zheng et al., 2019). In general, formulating and training a DNN model to analyze driver injury severity is challenging for several reasons. First, as claimed in previous studies, these neural network-based models behave as black boxes in which they do not provide the interpretable parameters we get when using statistical models (Abdelwahab and Abdel-Aty, 2002; Lord and Mannering, 2010; Mannering et al., 2020; Savolainen et al., 2011). Though several approaches proposed to represent model interpretability and explainability (see reviews in Guidotti et al. (2018)), these interpretation methods can hardly be applied to severity analysis of driver injury. These approaches are mostly designed for models fulfilling different pattern-recognition tasks, where the input data is continuous pixel-level information. However, in driver injury severity analysis, each variable owns the physical meaning, and some variables are mutually exclusive, especially for the dummy variables. Second, due to the randomly initialized weights and local optimized training algorithm, it has been observed that the training results of multiple runs are usually different. In contrast, these training results may provide similar performance, e.g., predictive accuracy. In this case, some variables may be essential in one run but not in the other run. A quick solution for this issue is to employ a fixed seed for the initial weight generation. However, in injury severity analysis domain, it is understandable that different impact factor on driver injury severity is interpretable. Accordingly, variables in multiple training runs shall provide similar impacts. Third, overfitting has been one of the commonly criticized problems in employing DNN approaches. Advanced techniques, such as regularization and dropout, can be applied to mitigate overfitting. Last but not least, unobserved heterogeneity and temporal instability shall be considered in driver injury severity analysis using DNN approaches.

2.3. Summary

Recent studies on crash modeling, impact factor analyses on crash injury severity, and other critical issues in the crash analysis were reviewed in this section. In this study, the project team will to propose a fusion convolutional neural network model with the random term (FCNN-R) for driver injury severity analysis. More specifically, we apply the fusion convolutional neural networks to investigate the relationships between the impact factors and driver injury severity. The unobserved heterogeneity across different crash records is illustrated using a random error term with zero means. Marginal effect analysis is applied to uncover the essentiality of each variable for driver injury severity. In addition, we also developed hierarchical Bayesian random parameters models with various spatiotemporal interactions to address this issue. Selected for analysis are the yearly county-level alcohol/drug

7

impaired-driving related crash counts data of three different injury severities including minor injury, major injury, and fatal injury in Idaho from 2010 to 2015.

CHAPTER 3.   FUSION CONVOLUTIONAL NEURAL NETWORK DEVELOPMENT

In this chapter, a fusion convolutional neural network with random term (FCNN-R) model is proposed for driver injury severity analysis. The proposed model consists of a set of sub-neural networks (sub-NNs) and a multi-layer convolutional neural network (CNN). More specifically, the sub-NN structure is designed to deal with categorical variables in crash records; multi-layer CNN structure captures the potential nonlinear relationship between impact factors and driver injury severity outcomes. Seven-years (2010-2016) of single-vehicle crash data are used to evaluate the performance of the proposed fusion convolutional neural network and analyze the driver injury severity. Models with different CNN layers are tested using the validation set, as well as various model layouts with and without a dropout layer or regularization term in the objective function. It is found that different model layouts provide consistent predictive performance. With the limited training data, more CNN layers result in the prematurity of the training procedure. The dropout layer and the regularization technique help improve the stability of the effects of different variables. The proposed model outperformed other five typical approaches in the predictability comparison. Moreover, a marginal effect analysis was conducted to the proposed FCNN-R model, the FCNN model and the mixed multinomial logit model. It shows that the proposed FCNN-R model can be used to uncover the underlying correlations similar to the traditional statistical models. Additionally, the temporal stability of the proposed FCNN-R approach is discussed based on the model performance in different years. Future research is recommended to include more information for improving the universality of the proposed approach.

3.1.   Data

Single-vehicle crash data were acquired from the Washington State Department of Transportation (WDOT) to illustrate the proposed FCNN-R model for driver injury severity analysis. Note that a single-vehicle crash in this study refers to a single-motor-vehicle crash with no other traffic objects. A dataset of crash records from 2010 to 2016 was extracted from traffic crash records. Four types of crash data are included: general crash information, such as crash type, crash timestamp, and crash location; driver information, such as driver injury severity, age, gender, seat belt usage, license status, insurance status, and sobriety conditions; vehicle information, involving vehicle type, vehicle age, and airbag condition; and environmental data, such as roadway type, roadside condition, speed limits, lighting condition, weather condition, road surface condition, and some other roadway characteristics.

Special care was conducted to screen out incomplete and outlier data to enhance data quality. For instance, the crash records with obviously incorrect information, such as drivers ages younger than 5, were removed from this study dataset. Moreover, similar variables were carefully examined and combined. For example, roadway type and road function class in the original dataset were both related to the road segment categories. Road function class was selected in this study as it classified the roadway segments into four categories: interstate, principal, minor arterial, and major arterial. Some continuous variables, such as driver's age, vehicle's age, and speed limits, were categorized based on traffic safety research experience (Chen et al., 2016; Guo et al., 2019; Li et al., 2018, 2019; Wu et al., 2016b). In total, 31115 driver injury records with 24 categorical variables were extracted, including 131 fatalities, 534 serious injuries, 5959 minor injuries, and 24491 no injuries. To maintain a statistically

meaningful sample size, three-driver injury severity levels were applied, e.g., no injury (N), minor injury (M), and severe and fatality injury (S/F). The descriptive statistic of the dataset is illustrated in Table 3-1.

Table **3-1** Variable Definitions and Descriptive Statistics

Variables	Values	Driver Injury Severity						Total
		N	%	M	%	S/F	%	
GENERAL								
Urban	Yes	10556	78.86%	2577	19.25%	253	1.89%	13386
	No	13935	78.60%	3382	19.08%	412	2.32%	17729
Season	Spring	4743	76.50%	1295	20.89%	162	2.61%	6200
	Summer	6060	76.73%	1610	20.38%	228	2.89%	7898
	Fall	6611	79.34%	1552	18.62%	170	2.04%	8333
	Winter	7077	81.49%	1502	17.30%	105	1.21%	8684
Weekend	Yes	8896	79.27%	2084	18.57%	242	2.16%	11222
	No	15595	78.39%	3875	19.48%	423	2.13%	19893
Object	Fixed	13996	78.26%	3487	19.50%	400	2.24%	17883
	Animal	5765	94.83%	293	4.82%	21	0.35%	6079
	Overturn	1937	57.00%	1306	38.43%	155	4.56%	3398
	Runoff	2793	74.38%	873	23.25%	89	2.37%	3755
Movement	Moving	21907	79.01%	5227	18.85%	594	2.14%	27728
	Turning	1082	80.75%	235	17.54%	23	1.72%	1340
	Parking	166	62.88%	77	29.17%	21	7.95%	264
	Backing	23	92.00%	1	4.00%	1	4.00%	25
	Merging	57	83.82%	11	16.18%	0	0.00%	68
	Out control	506	80.06%	120	18.99%	6	0.95%	632
	Lane change	750	70.89%	288	27.22%	20	1.89%	1058
DRIVER								
Age	(0,24]	14794	80.56%	3249	17.69%	321	1.75%	18364
	(24,45]	5430	76.33%	1504	21.14%	180	2.53%	7114
	(45,65]	3059	75.44%	874	21.55%	122	3.01%	4055

Variables	Values	Driver Injury Severity						Total
		N	%	M	%	S/F	%	
	Above 65	1208	76.36%	332	20.99%	42	2.65%	1582
Gender	Male	12707	80.63%	2714	17.22%	338	2.14%	15759
	Female	11784	76.74%	3245	21.13%	327	2.13%	15356
Sobriety	Impaired	1228	59.07%	652	31.36%	199	9.57%	2079
	Not impaired	300	69.93%	119	27.74%	10	2.33%	429
	No drink	22017	80.90%	4835	17.77%	362	1.33%	27214
	Other	946	67.91%	353	25.34%	94	6.75%	1393
Belt	Not Used	1631	54.37%	1012	33.73%	357	11.90%	3000
	Used	22860	81.31%	4947	17.60%	308	1.10%	28115
License	Yes	24221	78.85%	5838	19.00%	660	2.15%	30719
	No	270	68.18%	121	30.56%	5	1.26%	396
Liability	Yes	20709	81.14%	4413	17.29%	400	1.57%	25522
	No	3782	67.62%	1546	27.64%	265	4.74%	5593
VEHICLE								
Age	[0,4)	3234	84.73%	536	14.04%	47	1.23%	3817
	[4,8)	4799	82.39%	934	16.03%	92	1.58%	5825
	[8,12)	6398	79.61%	1490	18.54%	149	1.85%	8037
	[12,16)	5193	76.89%	1417	20.98%	144	2.13%	6754
	Above 16	4867	72.84%	1582	23.68%	233	3.49%	6682
Type	Passenger car	12068	78.71%	2959	19.30%	305	1.99%	15332
	Pickup	11648	79.90%	2635	18.08%	295	2.02%	14578
	Truck & Bus	351	80.88%	76	17.51%	7	1.61%	434
	Other	424	54.99%	289	37.48%	58	7.52%	771
Ejection	Totally	14	4.56%	133	43.32%	160	52.12%	307
	Partially	385	53.70%	251	35.01%	81	11.30%	717
	No	24092	80.06%	5575	18.53%	424	1.41%	30091
Airbag	Deployed	3209	60.15%	1880	35.24%	246	4.61%	5335
	Not deployed	15243	84.54%	2615	14.50%	173	0.96%	18031

Variables	Values	Driver Injury Severity						Total
		N	%	M	%	S/F	%	
	No airbag	6039	77.93%	1464	18.89%	246	3.17%	7749
ENVIRONMENT								
Road Type	Major	14054	78.62%	3404	19.04%	418	2.34%	17876
	Minor	2420	77.91%	596	19.19%	90	2.90%	3106
	Express	2692	79.27%	654	19.26%	50	1.47%	3396
	Interstate	5325	79.04%	1305	19.37%	107	1.59%	6737
Weather	Clear	13045	77.39%	3382	20.06%	430	2.55%	16857
	Overcast	4201	79.23%	982	18.52%	119	2.24%	5302
	Rain	4587	79.44%	1095	18.96%	92	1.59%	5774
	Snow	2531	83.92%	463	15.35%	22	0.73%	3016
	Wind	127	76.51%	37	22.29%	2	1.20%	166
Surface	Dry	13509	77.44%	3451	19.78%	484	2.77%	17444
	Wet	6507	79.38%	1553	18.95%	137	1.67%	8197
	Snow	2560	84.77%	443	14.67%	17	0.56%	3020
	Ice	1915	78.04%	512	20.86%	27	1.10%	2454
Lighting	Daylight	11886	77.38%	3162	20.59%	312	2.03%	15360
	Twilight	1392	77.94%	361	20.21%	33	1.85%	1786
	Dark light	3889	77.78%	994	19.88%	117	2.34%	5000
	Dark no light	7324	81.66%	1442	16.08%	203	2.26%	8969
Road Characteristics	Level	14043	78.62%	3432	19.21%	387	2.17%	17862
	Grade	9757	78.74%	2376	19.17%	259	2.09%	12392
	Hill & Sag	691	80.26%	151	17.54%	19	2.21%	861
Speed Limit	[5, 30]	2912	80.07%	665	18.28%	60	1.65%	3637
	(30, 60]	7708	77.64%	1940	19.54%	280	2.82%	9928
	Above 60	13871	79.04%	3354	19.11%	325	1.85%	17550
Medium Type	Single	3646	80.49%	824	18.19%	60	1.32%	4530
	Not divided	8666	77.92%	2155	19.38%	301	2.71%	11122
	Marked	2358	79.18%	550	18.47%	70	2.35%	2978

Variables	Values	Driver Injury Severity						Total
		N	%	M	%	S/F	%	
	Barrier	9614	78.59%	2393	19.56%	226	1.85%	12233
Work zone	Yes	338	80.48%	72	17.14%	10	2.38%	420
	No	24153	78.69%	5887	19.18%	655	2.13%	30695

3.2. Methodology

In this section, we present a fusion convolutional neural network for analyzing and predicting the driver injury severity in highway single-vehicle crashes. The proposed FCNN-R model includes two components: a set of sub-neural networks dealing with the input issue of various categorical variables and a deep convolutional neural network capturing the potential nonlinear relationship among the impact factors and driver injury severity outcomes. A merging layer is applied to connect the two parts. Additionally, the procedure for the marginal effect analysis considering the mutual exclusion among variables is also described.

3.2.1. MNL model

As introduced in the data description, several variables are incorporated into the model for each crash record. In most machine learning related crash analysis, the information is imported using a single data input layer (Zeng et al., 2016b; Zeng and Huang, 2014), or using separated sub-models based on their spatiotemporal patterns (Bao et al., 2019a). However, it is noted that most of the crash characteristics are categorical variables or say dummy variables. As shown in Figure 3-1(a), one categorical variable x_{ij}, i.e., the jth characteristic for ith crash records, is associated with a one-hot coding vector. Since each neuron unit performs a linear operator, zero inputs do make interactions with all the other variables, e.g., influence the model outputs via the bias term b and possible nonlinear activation function. In the other word, these un-occurring alternatives affect the crash output, which do not conform to the crash mechanism. All the alternative indicators would be treated equally as well as the alternative indicators from other categorical variables. However, in most traditional statistic models (such as the logit models, the probit models, and their variants), these dummy variables are linear linked and zero input makes zero influence on the utility value. To deal with this unrealistic issue, e.g., the parallel influence of alternatives from different variables, a fusion structure is proposed, as shown in Figure 3-1(b). For each categorical variable, a sub-neural network (sub-NN) is proposed to deal with relationships among the alternatives within a variable. A combination of different alternatives within a variable only affects the value of the sub-NN's output. Moreover, as shown in Figure 3-1(b), a random generator is designed in the proposed fusion structure. In this case, unobserved heterogeneity across the crash records is captured by specifying a random parameter for the crash record, which is similar to the standard random parameter model. The outputs of the sub-NNs and the random generator are then concatenated into one dense vector using a feature merging layer. The model layouts used in each part are briefly explained as follows.
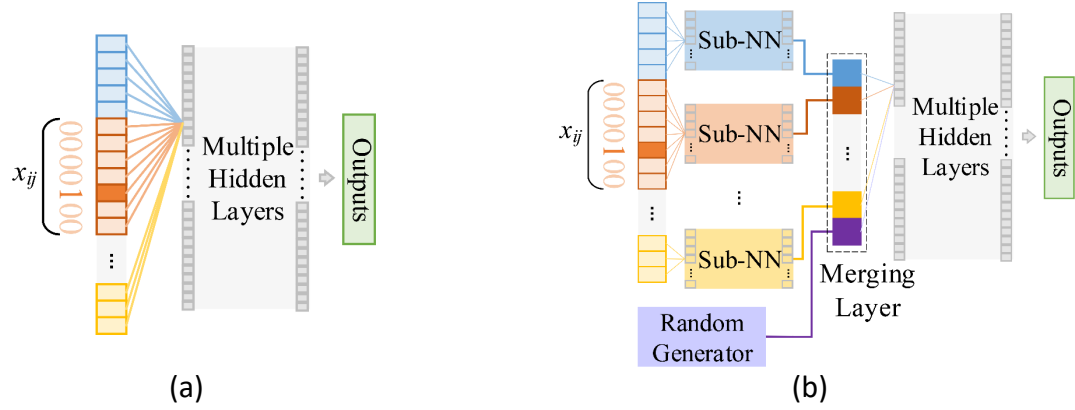
Figure 3-1 Input structure of crash characteristics: (a) traditional mode; (b) fusion structure.

1) *Input Structure for Crash Characteristics*

In this study, twenty-three sub-NNs are employed to capture the relationship among all the components for each variable, respectively. The underlying interaction is mainly performed via a multi-layer structure, as shown in Figure 3-2. In the sample layout for three dense layers, the first two dense layers consist of a set of hidden cells connecting an activation function, respectively. As shown in Figure 3-2, w_{ik}^m and b_k^m indicate the weights and the bias associated with the kth cell in mth hidden layer. Parametric rectified linear units (PReLU) are used as the activation function, as follows.

$$f(x) = \begin{cases} x & x \geq 0 \\ \alpha x & x < 0 \end{cases} \tag{3-1}$$

where α is a parameter for the neural network to figure out itself. Compared with the standard ReLU function, the PReLU is a benefit for no zero-slope parts and a faster learning rate (He et al., 2015). Following the two dense layers, the third dense layer consists of one cell indicating the variable output. It should be noted that though the same hidden layer structures in these sub-NNs are not necessary, the identical sub-NN layout is applied for simplification.
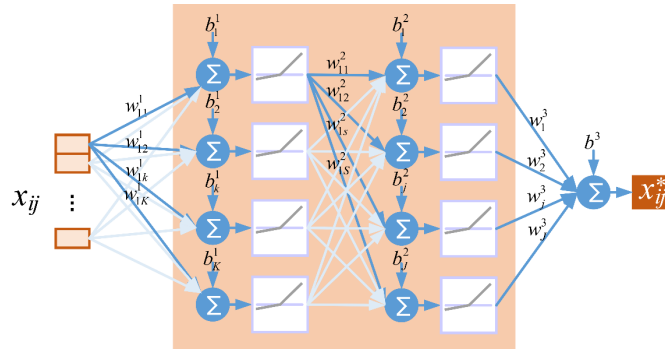
Figure 3-2 Sample layout for sub-neural network

The twenty-three variable outputs and the randomly generated parameter are concatenated into the 24-element vector via the merging layer, which represents the crash features extracted from the crash records. The random generator is an important and difficult point worthy of further study. In the present study, we tried several common distribution types, such as normal distribution, uniform distribution,

triangular distribution. No significant difference was identified. The possible reason of this phenomenon is that, in the DNN structure, the random generated variable interacts with other variables via numerous linear and non-linear operators. In this case, the assumption of the random term becomes less important since the parameters in the proposed DNN structure can vary across crash records. Finally, the vector is transferred into the multiple hidden-layer structures, described in the following section.

2) Multiple Hidden Layers

In this study, multiple hidden-layer structures are developed to explore the relationships among crash variables and driver injury severity and to predict driver injury severity outcomes for future crashes. The proposed structure consists of the convolutional layer and pooling layer, which are the two most important tools in the convolutional neural network (CNN). In the proposed structure, the convolutional layer consists of a set of learnable filters and is connected to a small patch of the input crash characteristics. Then, the filter slides from head to end of the input vector and computes the dot products between the weights in the filter and the associated patch. The pooling layer connecting to the convolutional layer reduces the feature size of crash information, which contributes to the problem of overfitting during training (Scherer et al., 2010). The max-pooling technique is applied in this study, which picks up the maximum value of neighboring elements as an output. It is one of the most commonly used pooling approaches (Boureau et al., 2010).

As shown in Figure 3-3, the 24-element vector is first input into a series of convolutional layers and pooling layers. Finally, the captured features of the crash record are flattened into a dense vector connecting to two additional dense layers for driver injury severity classification. It is easy to understand that the output layer contains three cells associated with the three injury severity levels, respectively, and the driver injury severity for the input crash record is the injury severity level with the most substantial output value.
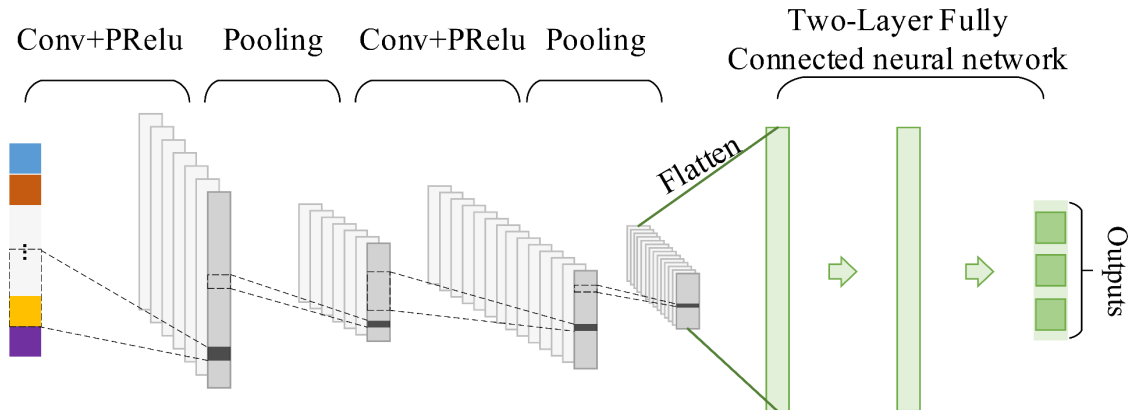

Figure 3-3 Structure of the proposed multiple hidden layers network

3) Objective Function

During the training process of the FCNN-R model, the objective is to minimize the cross-entropy loss between the model outputs and the real driver injury severity in each crash record, given as follows:

$$\min - \sum_{s} y_s^* \log\left(y_s\right)$$
(3-2)

15

where y_s^* is the label value for sth driver injury severity obtained from the original crash record, and y_s is the model prediction result for sth driver injury severity. To prevent overfitting, we further tested the dropout method with a probability of 0.5 at the second dense layer and the L2-norm regularization approaches by modifying the objective function as follow s (Srivastava et al., 2014):

$$\min - \sum_s y_s^* \log\left(y_s\right) + \lambda \left\|W\right\|_2^2 \tag{3-3}$$

where W indicates all the weights in the proposed FCNN-R model, and λ indicates the regularization parameter, which balances the bias-variance tradeoff. The training procedure is conducted with the keras module based on the open-source platform Tensorflow (v1.14). Additionally, to evaluate the applicability of the proposed FCNN-R model, two measurements, i.e., the prediction accuracy rate (PAR) and false positive rate (FPR), are employed to evaluate the performance of different driver injury severity levels, as follows.

$$PAR_S = \frac{TP_S}{FN_S + TP_S} \tag{3-4}$$

$$FPR_S = \frac{FP_S}{FP_S + TN_S} \tag{3-5}$$

where TP_s, FN_s, FP_s, and TN_s are given in the following confusion matrix in Table 2.

Table 3-2 Confusion Matrix for Predictive Performance of ith Driver Injury Severity

True Condition	Prediction Result	
	sth injury severity	Not sth injury severity
sth injury severity	True Positive (TP_s)	False Negative (FN_s)
Not sth injury severity	False Positive (FP_s)	True Negative (TN_s)

3.2.2. Marginal Effect Analysis

Some of the sensitivity analysis methods have been proposed to uncover the effects of different input information on the network outputs, such as the weights method, the partial derivation method, the randomization approach and rule extraction approaches (Dimopoulos et al., 1995; Garson, 1991; Hailesilassie, 2016; Olden and Jackson, 2002; Zeng et al., 2016b). The weights method proposed in Garson (1991) is relatively easy to implement but can hardly deal with the nonlinear activation function widely used in DNN models. The partial derivation method applied in Dimopoulos et al. (1995) improved the sensitivity analysis by multiplying the weight and the partial derivation of each activation function concerning its input. However, the partial derivation is required at each neuron cell. As a result, with the increasing network depth and model complexity, the computation needed for the partial derivation method is extensive.

In the present study, a marginal effect approach, which has been applied in many driver injury severity studies (Keramati et al., 2020; Yu et al., 2021), is modified to illustrate the significance of different variables via the proposed FCNN-R model. In the present case, the observed variables are all categorical variables. To uncover the impacts of the rth alternative of categorical variable x_{ij}, the jth variable for ith

crash record, we examine the change in model outputs due to a change in the binary status of the alternative as follows (i.e., a switch from a pre-determined baseline condition to the specific alternative):

$$M_{x_{ij}^r}^{O_{si}} = O_{si}\left[\text{given } x_{ij}^r = 1\right] - O_{si}\left[\text{given } x_{ij}^0 = 1\right] \tag{3-6}$$

where O_{si} is the output value associated with sth driver injury severity for ith crash record; $M_{x_{ij}^r}^{O_{si}}$ is the marginal effect for rth alternative indicator of jth variable in ith crash record; x_{ij}^0 represents the pre-determined baseline condition for jth categorical variable. The marginal effects in Equation (6) may be different for different individual crash records and each injury severity levels. To measure the impacts of variables on the entire dataset, the average marginal effect $\overline{M}_{jr}^s$ is calculated and reported. Moreover, to taking the random generator into consideration, multiple runs are conducted, as follows.

$$\overline{M}_{jr}^s = \frac{1}{HN}\sum_{h=1}^{H}\sum_{i=1}^{N} M_{x_{ij}^r}^{O_{si}} \tag{3-7}$$

where H is the number of multiple runs, and N is the number of crash records. Note that, in the present study, the marginal effect analysis was conducted for two purposes in the following section. Firstly, the stability of model training results is illustrated by comparing the signs of average marginal effects of different impact factors in multiple runs. Secondly, comparisons were conducted between the proposed FCNN-R model and a widely recognized statistic model, e.g., the mixed logit model, to reveal the explainability of the proposed model. Although the analysis results are data-driven and cannot comprehensively interpret the effects, these numerical results showed that the proposed FCNN-R model captures the capability of interpreting the effects of observed factors on each severity level, just like the traditional statistical model does.

3.3. Result

This section presents the performance of the proposed FCNN-R model using 7-years of highway single-vehicle crash data. Note that, besides the simple FCNN-R model (shown in Figure 3-3), we also tested the FCNN-R model with dropout layer and/or regularization term, i.e., the four types of model layouts are:

- I: simple FCNN-R model

- II: FCNN-R model with a dropout layer

- III: FCNN-R model with L2-norm regularization term in the objective function

- IV: FCNN-R model with dropout layer and L2-norm regularization term in the objective function

The best layout of the proposed FCNN-R model was then compared with two widely used statistical methods, i.e., the multinomial logit (MNL) model and the mixed multinomial logit (MMNL) model, and three neural network-related approaches, including the neural network (NN) model, the convolutional neural network (CNN) model, and the fusion convolutional neural network (FCNN) model. In order to investigate the explainability of the proposed FCNN-R model, the marginal effects of the significant

factors in the MMNL model and the proposed FCNN-R model were compared. Additionally, the temporal stability of the proposed model was tested with the 7-year crash data. The coding and execution of the statistical models were accomplished using NLogit Version 5, and the neural network-related approaches were implemented on the same platform as the proposed FCNN-R model.

The selected dataset is divided into three parts, including the Training set, Validation set, and Test set. More specifically, a total of 9000 crash records (around 30% of the whole dataset) is randomly selected from the 7-year dataset and is kept aside as the Test set. After this, we randomly choose 80% of the rest crash records to be the Training set, while the remaining 20% is the Validation set. The difference between the Validation set and the Test set is that the Validation set is used to provide an unbiased evaluation for tuning model hyper-parameters (parameters for model layouts), while the Test set is used to evaluate the final model.

3.3.1. Model Specification

In the procedure of model specification, we mainly focused on tuning the hyper-parameters of the proposed FCNN-R model, as well as choosing the best layout mentioned above. In this case, the Training set and Validation set are applied. The proposed FCNN-R model with different model layouts, i.e., well trained FCNN-R model with a different number of CNN layers, are listed in Table 3-3. Since there are no general rules for directing the hyper-parameters setting, the selection of hyper-parameters mainly relies on the empirical experience evidence and previous works of literature (Bao et al., 2019a; Yu, H. et al., 2020a). Expressly, the filter size of the convolutional layer in this study is set as (3, 1), and the filter size of the max-pooling layer is set as (2, 1). The depths of the convolutional layer are tested by assigning different values of 8, 16, 24, 32, 40, and 48 to achieve an optimal result and for the sub-NNs, the different hidden cell sizes of 16, 32, 64, 128, are employed to determine the optimal dimensions of hidden cells in crash data input. Note that in the specification of the traditional statistic models, such as the multinomial logit, a correlation test is important and useful before the stepwise variable selection. By conducting the correlation test, closely correlated variables shall not be involved in the model at the same time. However, in the present study, though some variables may be correlated, these variables may contribute different information in a crash record. In this case, the correlation test is omitted here.

As shown in Table 3-3, the model layouts with a different number of CNN layers provide comparable results for both the accuracy and predictive performance in different injury severity outcomes. More specifically, the model performance increases as the number of CNN layers rises from 2 to 3 but slightly decreases as the number of CNN layers rises from 3 to 5. One possible explanation is with the limited input information (24-element vector), more CNN layers result in the prematurity of the Adam Optimizer applied in this study. It is found that among the four different model layouts, type I layout, i.e., the simple FCNN-R model provided the best accuracy in both training and validation sets. However, it is noticed that the dropout technique and the regularization technique do improve the problem of over-fitting, as the accuracy differences between training and validation sets are reduced for a different number of CNN layers, indicating that the robustness of the proposed FCNN model is improved with the dropout layer or the regularization term in the objective function. Similar trends can also be observed based on the predictive performance measurements, i.e., PAR and FPR indices. Following the definition of PAR and FPR indices, it is clear that a model with higher PAR and lower FPR performs better. In light of this, a roughly designed summary score C^l is calculated for a model layout, as follows:

$$C^l = \sum_s PAR_s^l - FPR_s^l \qquad (8)$$

where PAR_s^l and FPR_s^l is the *PAR* and *FPR* indices associated with the *s*th driver injury severity of model layout *l*. Based on Equation (8), the simple FCNN-R model, i.e., layout type I, with 3 CNN layers, performs best, which is consistent with the accuracy performance.

Table 3-3 Results of Different Model Layouts

Number of CNN Layers	Model Layout	Accuracy		Performance by Driver Injury Severity						Summary Score
		Training	Validation	N		M		S/F		
				PAR	FPR	PAR	FPR	PAR	FPR	C
2	I	0.820	0.802	86.7%	76.2%	54.4%	4.2%	72.9%	0.2%	133.4%
	II	0.817	0.793	87.4%	79.5%	47.6%	4.4%	63.8%	0.3%	114.6%
	III	0.797	0.806	88.9%	79.5%	48.9%	2.6%	59.4%	0.3%	114.8%
	IV	0.799	0.792	89.2%	89.4%	41.1%	1.7%	54.3%	0.4%	93.1%
3	I	0.838	0.827	88.5%	68.1%	59.2%	3.3%	79.4%	0.2%	155.5%
	II	0.817	0.814	88.9%	72.4%	52.8%	3.7%	63.8%	0.2%	129.2%
	III	0.801	0.809	89.4%	80.2%	49.1%	2.3%	52.9%	0.2%	108.7%
	IV	0.798	0.808	89.5%	80.7%	48.4%	2.3%	48.3%	0.2%	103.0%
4	I	0.838	0.825	88.4%	69.2%	58.6%	2.8%	79.2%	0.5%	153.7%
	II	0.819	0.818	88.7%	73.9%	56.1%	2.8%	59.1%	0.2%	127.0%
	III	0.800	0.807	88.9%	79.5%	50.3%	2.7%	51.4%	0.1%	108.3%
	IV	0.796	0.806	89.4%	82.5%	47.7%	2.1%	50.1%	0.2%	102.4%
5	I	0.832	0.811	88.0%	66.5%	53.6%	5.3%	73.2%	0.5%	142.5%
	II	0.817	0.807	88.8%	79.7%	49.8%	2.9%	59.2%	0.0%	115.2%
	III	0.798	0.804	89.3%	82.8%	46.7%	2.1%	58.2%	0.3%	109.0%
	IV	0.792	0.800	89.7%	87.3%	43.0%	1.8%	52.9%	0.0%	96.5%

3.3.2. **Stability of Marginal Effects**

The marginal effect analysis, described in Equation (3-7), is applied to the trained models with three CNN layers in different model layouts, i.e., layout I-IV. The signs of the average marginal effects in multiple training runs for different variable are illustrated in Figure 3-4. More specifically, 12 sub-figures are involved showing the results for different layout type-injury severity pairs; each sub-figure consists of 56*100 pixels, where 56 is the number of various variable indictors (79 variables shown in Table 3-1 minus 23 pre-specific baseline condition), and 100 is the number of multiple training runs with different

random starting weights; and the meaning of the three colors, i.e., red, blue, and white, applied in each sub-figure represent positive, negative and zero average marginal effect values, respectively. Different from the marginal effect analysis for the traditional statistical model, which focuses on the effects of various impact facts on driver injury severity outcome, the comparison results presented in Figure 3-4 mainly emphasize whether the effect of each impact factor is stable to each injury severity outcome in different runs.
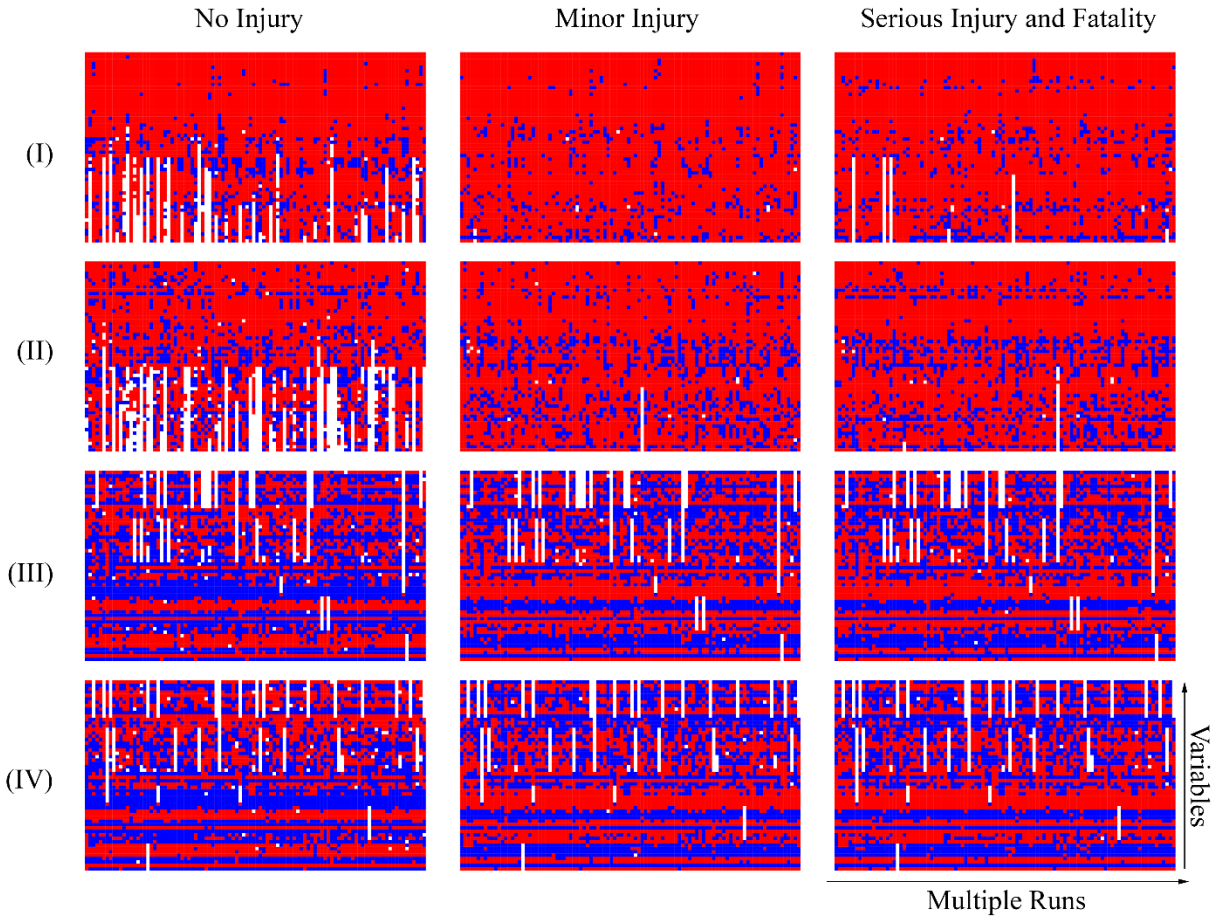
Figure 3-4 Comparison results of a marginal-effect based stability analysis with different layouts

As shown in Figure 3-4, clear stripe ribbons can be observed in sub-figures associated with model layouts with regularization term in the objective function, i.e., type III and type IV layouts, indicating the sign stability of the elasticities across multiple runs. Moreover, it is also found that the dropout technique, i.e., type II layout, slightly improves the model stability of the marginal effect, compared to the simple FCNN-R model. In summary, based on the test results, the regularization and dropout techniques both improve the stability of the model interpretation. Further analysis on the marginal effects is presented in the following section.

3.3.3. Model Comparisons

1) Predictive Performance

The predictive performance of the five state-of-art approaches, including the multinomial logit (MNL) model, the mixed multinomial logit (MMNL) model, the neural network (NN) model, the convolutional neural network (CNN) model, and the fusion convolutional neural network (FCNN) model, are compared to the proposed FCNN-R model, as shown in Table 3-4. The five approaches in this study are briefly described as follows:

(1) MNL: the MNL method is one of the most disseminated approaches in driver injury severity analysis. Since the MNL model specifications have been well documented in many existing studies, the development of the MNL model is omitted. Based on maximum likelihood estimation, parameters for significant impact factors are calibrated with the training dataset. The performance of driver injury classification is obtained by applying the model to the testing dataset.
(2) MMNL: the mixed multinomial logit model is more flexible than the MNL method. It takes the heterogeneity among different crashes into consideration. In this study, parameters with random effects or fixed effects, are selected using the step-wise approach, and distribution models, including normal, triangle, and uniform, are examined.
(3) NN: the NN model applied in this study involved a single hidden layer with 256 neuron cells and is fitted with multiple random starting weights.
(4) CNN: the CNN model used in this study employed the layout, as shown in Figure 3-3. The only difference is that the input data in Figure 3-3 come from the sub-NN nets, while the original crash information is transferred into the model directly.
(5) FCNN: the FCNN model is almost the same as the proposed FCNN-R model except for the random term. The FCNN model is conducted to evaluate the impacts of the random term in the proposed FCNN-R model.

Table 3-4 Comparison of Performance with Different Models

Model	Accuracy		Performance						Summary Score
	Training	Test	N		M		S/F		
			PAR	FPR	PAR	FPR	PAR	FPR	C
MNL	0.793	0.791	97.5%	82.7%	12.9%	3.0%	17.4%	0.3%	41.8%
MMNL	0.812	0.809	96.8%	73.9%	20.8%	3.1%	19.6%	0.3%	59.9%
NN	0.843	0.815	90.3%	70.3%	48.5%	4.2%	43.9%	0.6%	107.6%
CNN	0.830	0.813	89.1%	72.3%	50.9%	4.2%	54.4%	0.4%	117.5%
FCNN	0.836	0.826	89.4%	70.6%	54.8%	3.2%	71.9%	0.3%	142.0%
FCNN-R	0.836	0.832	89.4%	68.7%	57.5%	2.9%	77.2%	0.2%	152.3%

As shown in Table 3-4, it is found that the proposed FCNN-R model outperformed the five typical approaches in the testing accuracy and the summary score *C* in Equation (3-8), as expected, followed by

the FCNN, the CNN, the NN, the MMNL, and the MNL. It shows that the MNL approach provided the highest PAR_N value over the other methods, including the proposed FCNN-R model. However, it is noted that the PAR_M and PAR_S for the MNL approach are quite low. It shows that the MNL tends to classify most crashes as no injury (N), which results in high percentages in both PAR_N and FPR_N.

It is of interest to take a further look at the four neural network-based approaches. The FCNN-R outperforms the other three methods in all the *PAR* and *FPR* indices. Though, in general, the CNN model is a benefit for capturing hierarchical features among the input information, there is no significant difference between the NN and CNN models in their predictive performances. One possible explanation is that the convolutional filters are not quite suitable for the categorical variables with a different number of categories. The proposed fusion models with multiple sub-NNs improve the performance of the CNN model by dealing with the categorical variables separately. Compared to the FCNN model, the proposed FCNN-R model provides better performance in the test dataset, indicating that the random term improves the model robustness.

2) *Explainability of the FCNN-R model*

The MMNL has been one of the most widely applied analytic approach to investigate effect of impact factors with unobserved heterogeneity. In this section, we presented the marginal effect analysis conducted on the FCNN model, the proposed FCNN-R model and the MMNL model. Note that only the factors showing significant impacts at 95% level of confidence in the MMNL model specification are compared here. As shown in Figure 3-5, the marginal effects of 18 impact factors were illustrated. The red dots are the average marginal effects generated in multiple runs.

The explainability of the three models can be briefly discussed in two aspects, i.e., the means and the variances. For the means, all the signs of the average marginal efforts of these impact factors on different injury severity are almost the same, and the proposed FCNN-R model showed closer results to the MNNL model than the FCNN model. The findings indicate that the proposed FCNN-R model, as well as the FCNN model, is capable to capture the effects of the impact factors similar to the traditional models. With a few exceptions, the values of the marginal effects obtained from the proposed FCNN-R are nearly the same as these obtained from the MMNL model. The slight difference might be introduced by other impact factors, which are involved in the FCNN-R model, but removed from the MMNL model. For the variance, the average marginal effects obtained from the proposed FCNN-R fluctuate within certain ranges, which, to some extent, shows that the proposed FCNN-R model demonstrates the impact of the unobserved heterogeneity. In light of the fact that the FCNN model produces only a static average marginal effects, it can be concluded that the random term makes the proposed model possess the capability of capturing heterogeneity. Rigorous tests on the power of the demonstrating the unobserved heterogeneity for the proposed FCNN-R model are recommended in future research.
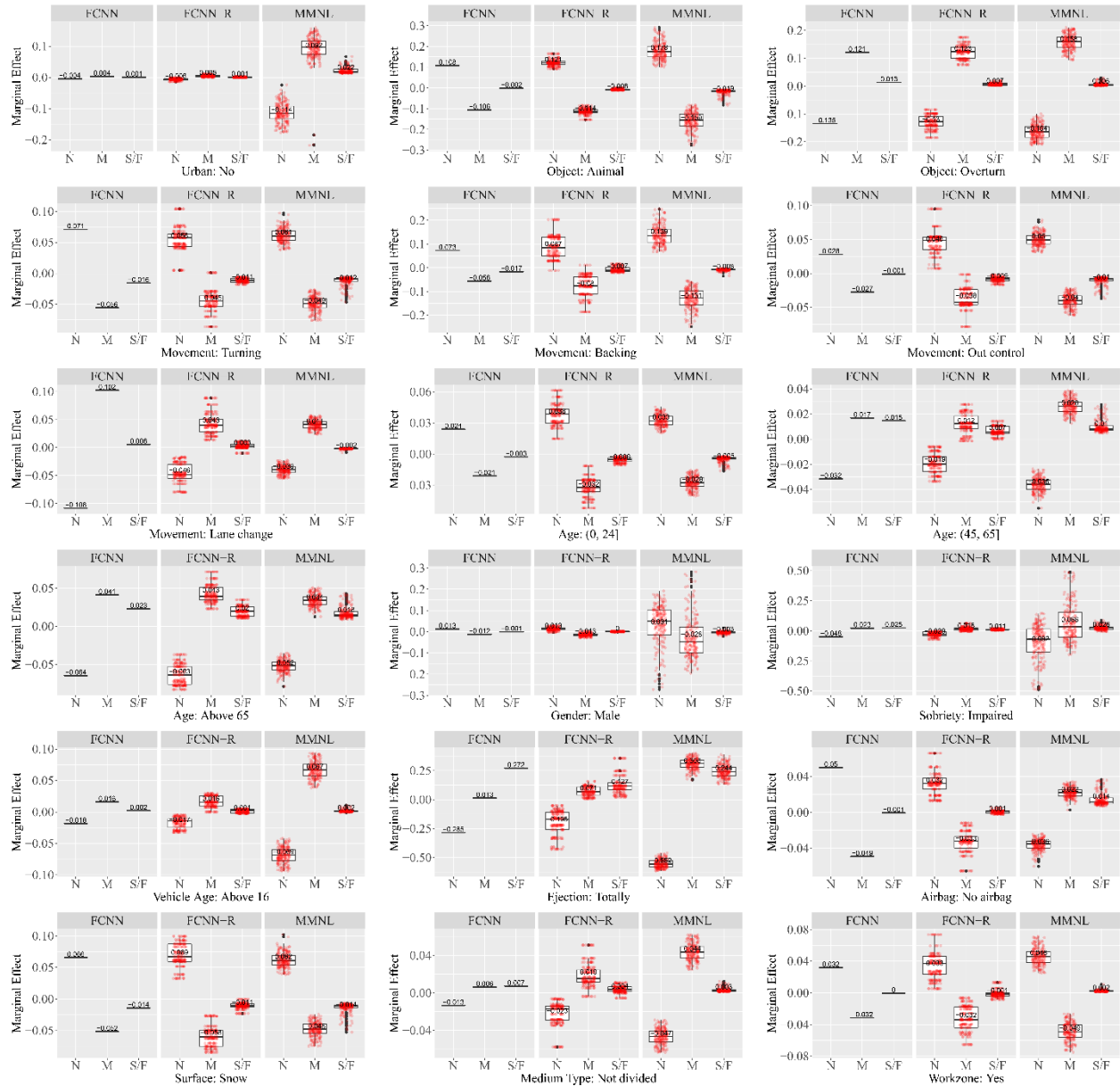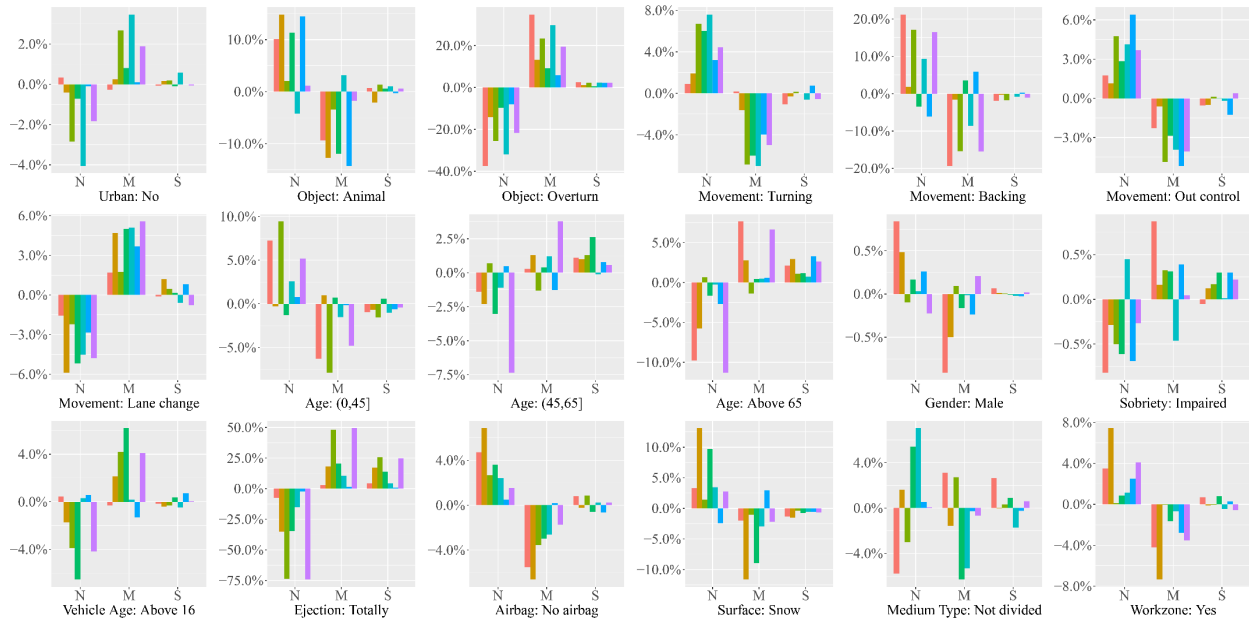
Figure 3-5 Marginal effects comparison of significant variables among the FCNN model, the proposed FCNN-R model and the MMNL mode

3.3.4. **Temporal Stability**

(a) Marginal effects
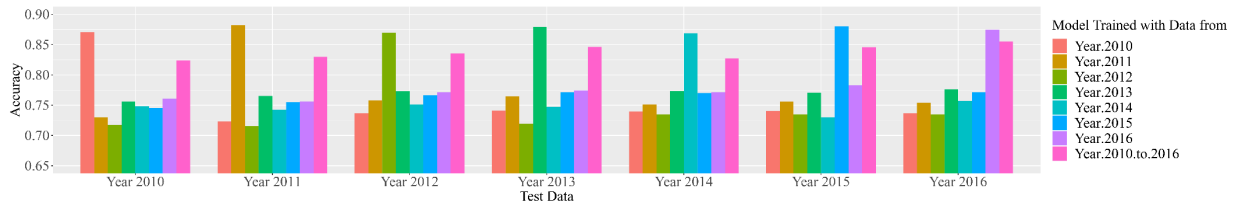
(b) Predictabilities

Figure 3-6 Performance of temporal stability for the proposed FCNN-R model from 2010 to 2016

In addition to the predictive performance and the marginal effects analysis presented above, the proposed model structure is trained using annual crash data from year 2010 to year 2016. Time-varying predictive performance and time-varying marginal effect estimations are illustrated in Figure 3-6. As shown in Figure 3-6(a), the time-varying marginal effect estimations for variables with significant impacts are compared across different years. It shows that among the 18 significant factors, only 2 variables, i.e., the overturn indicator and the totally ejection indicator, show perfect temporal stability, while other variables more or less show both positive and negative marginal effects on different injury severity levels. The time-varying marginal effects, especially for the changes between positive and negative, might be caused for two reasons, including insufficient data and temporal instability. Firstly, the limited crash data in each year restricts the accurate estimation of the marginal effects of the model on this impact factors. Secondly, the effect of these impact factors does change from year to year, such as the individual's safety attitude, the improvement of safety equipment, and their influence on driving behavior and crash outputs (Mannering, 2018).

As shown in Figure 3-6(b), the same color of the bars indicates that the model is trained using the same year's data. It is understandable that for each specific year, the model trained using the same year's

data performs best, followed by the model trained using all the crash data (from 2010 to 2016). The models trained using other years' data have slightly worse but comparable performance. The predictive performance is slightly different from intuitive cognition that the predictive performance may reduce as the time gap increases. With the proposed fusion convolutional neural network approach, the predictive accuracies fluctuate randomly within certain ranges from year to year. The findings indicate that: the proposed FCNN-R model captures the capability of demonstrating the possible temporal variation across the studying periods, and more data do improve the model performance on prediction tasks; and temporal instability influences not only the effects of various impact factors on crash injury outputs, but also the model predictive performance among different years. For future research, the model structure which considers time-varying interaction among variables, which can explain the potential temporal heterogeneity, is worthy of further investigation.

3.4. Summary

In this study, a DNN structure, *i.e.*, the FCNN-R model, is proposed for driver injury severity analysis. The proposed FCNN-R model consists of a set of sub-NNs and a multi-layer CNN. Specifically, multiple sub-NNs are proposed for various categorical variables input; a random term is designed in the input layer to capture unobserved heterogeneities across individual crash records; the multi-layer CNN model captures the potential nonlinear relationship among impact factors and driver injury severity outcomes. The proposed model is fed with single-vehicle crash records acquired from Washington State for the period of 2010 to 2016, including general crash information, driver information, vehicle information, and environmental information. The whole dataset is divided into three parts, i.e., the training, the validation, and the testing datasets. Different model layouts, i.e., different number of CNN layers and different techniques preventing from overfitting, are tested using the validation dataset. With the limited training data, more CNN layers result in the prematurity of the training algorithm applied in this study. Moreover, it is noted that the regularization and dropout techniques do improve the stability of the proposed model. However, they do not improve the predictive performance of the proposed model. The proposed FCNN-R model is compared with five typical approaches, i.e., the MNL, the MMNL, the NN, the CNN, and the FCNN model, using the test dataset. The comparison results indicate that the proposed model outperforms the other approaches in all the performance indices.

The comparison of the marginal effects between the proposed FCNN-R model and the MMNL model indicates that the DNN framework has the potential to capture the underlying relationship between various factors from vast data sources and driver injury severity outcomes. Once the model is well trained, the proposed FCNN-R can be used to not only predicting crash outcomes but also to estimate the effects of risk factors on injury severities. However, there exist several limitations of the proposed model. Firstly, the proposed model is only tested using single-vehicle crashes from the Washington States. For future research, the generalization and the transferability of the proposed mode shall be tested. Moreover, an improved model which allows absent variables should be pursued to improve the transferability of the proposed model for crash records with different variable sets. Secondly, the proposed model currently involves only crash records. We recommend including more information in the proposed model in a future study. Finally, advanced training algorithms for deeper models and more efficient model structures, such as the recurrent structures and the residual blocks, are of great interest and could be explored in the future.

CHAPTER 4. HIERARCHICAL BAYESIAN SPATIOTEMPORAL RANDOM PARAMETERS MODEL DEVELOPMENT

Unobserved heterogeneity, which has been recognized as a critical issue in crash frequency modelling, generates from multiple sources, including observable and unobservable factors, space and time instability, crash severities, etc. However, only a very limited body of research is dedicated to distinguish and simultaneously address all these sources of unobserved heterogeneity. In this study, hierarchical Bayesian random parameters models with various spatiotemporal interactions are developed to address this issue. Selected for analysis are the yearly county-level alcohol/drug impaired-driving related crash counts data of three different injury severities including minor injury, major injury, and fatal injury in Idaho from 2010 to 2015. The variables, including daily vehicle miles traveled (DVMT), the proportion of male (MALE), unemployment rate (UR), and the percentage of drivers of 25 years and older with a bachelor's degree or higher (BD), are found to have significant impacts on crash frequency and be normally distributed in certain crash severities. Significant temporal and spatial heterogenous effects are also detected in all three crash severities. These empirical results support the incorporation of temporal and spatial heterogeneity in random parameters models.

The rest of the chapter is organized as follows: Section 4.1 provides detailed descriptions of the data utilized. Model development is carefully illustrated in Section 4.2. Section 4.3 presents the model estimation results and corresponding discussions. Finally, the chapter is concluded in Section 4.4.

4.1. Data

The analyzed dataset from Idaho's 44 counties, which contains all alcohol/drug impaired-driving related crash records, was obtained from the Idaho Transportation Department. The geographic characteristics of these counties are shown in Figure 4-1. As shown in Figure 4-1, Idaho is divided into seven sub-regions based on their locations, elevations, climate conditions, population densities, and other geophysical and demographic characteristics. In the original dataset, crashes are classified into five categories by severity: fatal, major injury, minor injury, possible injury, and property damage only. According to the Idaho crash reports (Idaho Transportation Department, 2015), the economic cost of per occurrence of a minor injury, major injury, and fatal crash is almost 39, 142, and 2,967 times as much as that of property damage only crash, respectively. Considering the significant economic loss and casualties, fatal crashes, major injury crashes, and minor injury crashes are retained from the original dataset. After carefully removing all the incomplete and erroneous records, 4,926 alcohol/drug impaired-driving related crash records from 2010 to 2015 were selected and utilized in this research. Road and traffic-related factors are mainly extracted from the Idaho Transportation Department public records, Idaho Open Data Portal, Bureau of Transportation Statistics. A number of factors reflecting the demographic and socioeconomic features are also downloaded from the United States Census reports, Statistical Atlas, and Idaho Department of Labor. Some nominal and ordinal variables are converted into values for further analyzing. Table 4-1 presents the summary of variables of each county at each year, as well as major descriptive statistics of these variables, including mean, standard deviation (SD), minimum (Min), and maximum (Max). The numbers of minor injury crashes (MIC), major injury crashes (MAC), and fatal crashes (FAC), are selected as the dependent variables. The other variables in Table 4-1 are treated as explanatory variables and are widely used in previous macroscopic safety analyses (Chiou and Fu, 2015; Zeng et al., 2016; Huang et al., 2017). Subfigures (a), (b), and (c) in Figure 4-2 demonstrate the frequencies of minor injury, major injury, and fatal crashes aggregated from 2010 to 2015 in Idaho by

county (similar distributions were obtained for each year), respectively. It is clear that the highest values of all three crash severities are clustered around the counties of Ada in Region 4, Kootenai in Region 1, and Bingham in Region 7. The results are not surprising since these counties all have larger populations than other counties, and therefore they are associated with more crashes.

Table 4-1 Summary of Variables and Descriptive Statistics

| Variables	Definition	Mean	SD	Min	Max
MIC	Total number of minor injury crashes	9.37	28.72	0	94
MAC	Total number of major injury crashes	6.21	34.13	0	74
FAC	Total number of fatal crashes	3.12	3.92	0	21
DVMT	Daily vehicle miles traveled (by natural logarithms)	13.84	13.9	3.34	16.24
POP	Total population (by natural logarithms)	10.48	11.11	6.88	12.88
MALE	Proportion of male	50.90%	0.01	48.40%	55.30%
UR	Unemployment rate	3.11%	0.01	1.60%	9.50%
PAV	Pavement condition (Good=1, Fair=0.8, Poor=0.6, Very Poor=0.4)	0.84	0.18	0.71	0.92
LN	Number of lanes	2.38	0.11	2.15	3.02
BD	Percentage of 25 years and older with a bachelor's degree or higher	25.10%	0.23	6.90%	54.40%
INC	Median percentile of household income (USD, by natural logarithms)	10.75	9.70	10.38	11.07

Figure 4-1 Idaho County Map
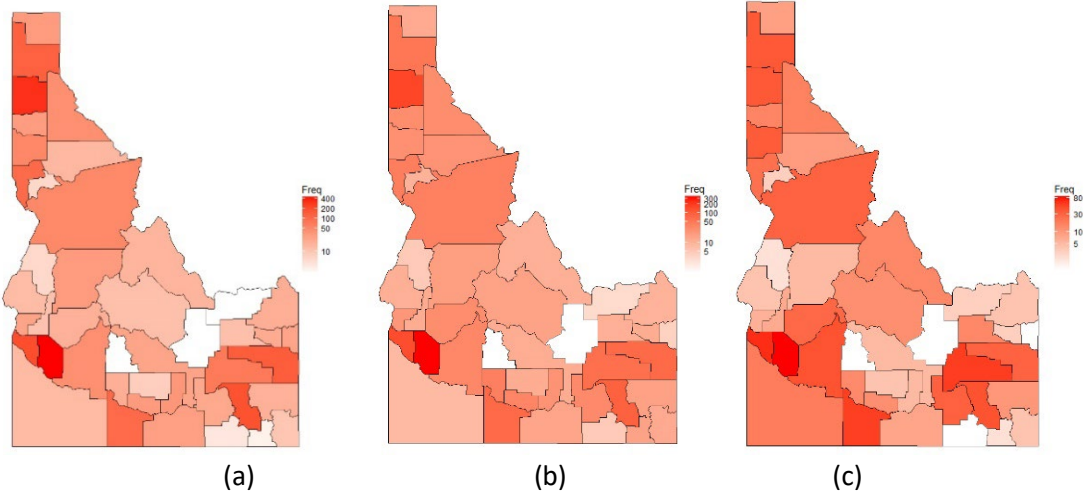
Figure 4-2 Frequencies of Three Severities of DUI Crashes from 2010 to 2015 in Idaho by County (a: Minor Injury Crash, b: Major Injury Crash, c: Fatal Crash)

4.2. Methodology

4.2.1. Model development

As noted in the last section, the crash frequency data is summarized in a formally defined region within a regular time intervals, i.e., in the county within each year in this study. Let y_{itk} denote the number of kth $(k = 1, \dots, K)$ injury level crashes in county i $(i = 1, \dots, n)$ and year t $(t = 1, \dots, T)$ with K injury severity levels. In the sequel, we assume that y_{itk} is a count arising from an associated mean crash frequency η_{itk}. Thus, the Bayesian modeling process contains two stages: (1) specifying a likelihood model for the vector of observed crash counts $\boldsymbol{y}$ given the vector of the mean crash frequency $\boldsymbol{\eta}$; (2) specifying a prior model over the space of possible $\boldsymbol{\eta}$'s. The Markov chain Monte Carlo (MCMC) algorithm yields a posterior for $\boldsymbol{\eta}$ given $\boldsymbol{y}$.

The likelihood model assumes that, given $\boldsymbol{\eta}$, the crash counts y_{itk} are conditionally independent Poisson variables, that is

$$y_{itk} \sim \text{Poisson}(\eta_{itk}) \qquad (4\text{-}1)$$

and η_{itk} has the decomposition

$$\log(\eta_{itk}) = \mu_k + \sum_{m=1}^{M} \text{X}_{mitk}^T \beta_{mitk} + \alpha_{tk} + \gamma_{tk} + \theta_{ik} + \phi_{ik} \qquad (4\text{-}2)$$

where μ_k is the intercept term, X_{mitk}^T is the covariate matrix of county i in time unit t, m $(m = 1, 2, 3, \dots, M)$ is the number of variables, and β_{mitk} is the corresponding regression coefficient vector of kth injury severity crash. β_{mitk} is assumed to follow a normal distribution, based on previous modeling experience and studies (Anastasopoulos and Mannering, 2009; Milton et al., 2008). Thus, this model is a random parameters model, and the variations are represented by allowing all regression coefficients to vary randomly from one observation to another. α_{tk} and γ_{tk} are temporal effects, representing

28

unspecified features of year t that respectively do or do not display temporal structure. Similarly, θ_{ik} and ϕ_{ik} represent unspecified features of county i that respectively do or do not display spatial structure.

Poisson serves as an approximation to a binomial distribution that some previous studies used to replace Poisson distribution (Musenge et al., 2013; Williams et al., 2018). If the crash counts are large enough then y_{itk} or $\sqrt{y_{itk}}$ can be assumed to approximately follow a normal density. However, partitioning crash counts by severity results in many small values of y_{itk} (including several zeros, especially for fatal crashes), so the Poisson model is more appropriate for analyzing our dataset.

Splitting up the overall temporal effect into structured effect and unstructured effect is due to some temporal effects may obey a strong yearly trend and others may be present only within one year. Similarly, the structured spatial effect can demonstrate the spatial variations across different counties, and the unstructured spatial is able to capture the spatial heterogeneity that presents locally. These treatments are rational since both the temporal and the spatial effects are usually a substitute for many unobserved influencing factors.

The Eq. (4-2), named as the main effect model, is completed by assigning prior distributions to the four temporal or spatial effects related blocks $\alpha_k = (\alpha_{1k}, \ldots, \alpha_{Tk})^T$, $\gamma_k = (\gamma_{1k}, \ldots, \gamma_{Tk})^T$, $\theta_k = (\theta_{1k}, \ldots, \theta_{nk})^T$, and $\phi_k = (\phi_{1k}, \ldots, \phi_{nk})^T$. Each prior is assumed to follow a (singular) multivariate Gaussian distribution with mean zero and precision matrix κK, where κ is an unknown scalar and K is a known structure matrix (Besag and Kooperberg, 1995; Clayton, 1996). Each block has a unique structure matrix K because the assumptions about the prior interrelationships between parameters are different within each block. The symbolic representation of these four blocks is given in Figure 4-3.
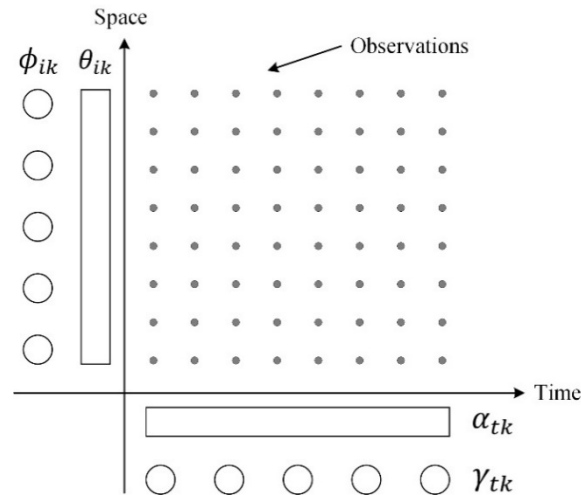
Figure 4-3 Symbolic Representation of the Main Effect Model (Rectangles Represent Prior Dependence, and Circles Represent Prior Independence)

For the structured temporal heterogeneity block, α_k, we adopt a global smoothness prior in which the temporal effects for neighboring years tend to be alike. Since we divided the crash frequency by year, therefore the observations are equidistant in terms of time. Generally, the simplest form of such models is the first order random walk approach with independent Gaussian increments (Besag, 1991; Clayton, 1996), such that

$$p(\alpha_k|\kappa_{\alpha_k}) \propto \exp(-\frac{\kappa_{\alpha_k}}{2}\sum_{t=2}^{T}(\alpha_{tk}-\alpha_{(t-1)k})^2) \tag{4-3}$$

and the corresponding structure matrix K_α can be given as

$$K_{\alpha_k} = \begin{pmatrix} 1 & -1 & & & & & \\ -1 & 2 & -1 & & & & \\ & -1 & 2 & -1 & & & \\ & & \vdots & \vdots & \vdots & & \\ & & & -1 & 2 & -1 & \\ & & & & -1 & 2 & -1 \\ & & & & & -1 & 1 \end{pmatrix} \tag{4-4}$$

The precision κ_{α_k} controls the degree of the smoothness of the structured temporal effect.

For the unstructured temporal heterogeneity block, γ_k, we assume exchangeability of the components by letting its corresponding matrix K_{γ_k} be an identity matrix, i.e., $K_{\gamma_k} = I$. In essence, the unstructured effects are i.i.d. Gaussian, thus

$$p(\gamma_k|\kappa_{\gamma_k}) \propto \exp(-\frac{\kappa_{\gamma_k}}{2}\gamma_k^2) \tag{4-5}$$

The structured spatial heterogeneity block θ_k, suggests that the counties that are closer to one another are likely to have common features affecting their crash frequency. In order to capture this heterogeneity, a Gaussian intrinsic conditional autoregression (ICAR) model can be adopted (Besag and Green, 1993), such that

$$p(\theta_k|\kappa_{\theta_k}) \propto \exp(-\frac{\kappa_{\theta_k}}{2}\sum_{j\in N_i}(\theta_{ik}-\theta_{jk})^2) \tag{4-6}$$

where j is a county that shares a common boundary with county i, and N_i is the set of all the neighborhoods of county i. The elements of the corresponding structure matrix, K_{θ_k}, are also related to the neighborhoods of county i. The diagonal entries k_{ii} equal to $\#N_i$, i.e., the number of all the counties that are geographically contiguous to county i. Besides, the non-diagonal elements $k_{ij}(j \neq i)$ are all set to be equal to -1, and all the other elements in K_{θ_k} are zero. This Markov random field prior is the spatial analogue of the random walk approach and also is non-stationary. Thus, the mean of θ_k is an average of function evaluations of neighboring counties. Again, the precision κ_{θ_k} has an impact on the degree of smoothness of this effect.

 Similarly, for the unstructured spatial heterogeneity block, ϕ_k, a common assumption is also that the parameters are i.i.d. Gaussian, thus

$$p(\phi_k|\kappa_{\phi_k}) \propto \exp(-\frac{\kappa_{\phi_k}}{2}\phi_k^2) \tag{4-7}$$

with the corresponding matrix $K_{\phi_k} = I$.

Therefore, the main effect model Eq. (4-2) is able to account for unobserved temporal and spatial heterogeneity in the crash frequency data. However, it is lack of the presence of time × space interactions due to its separable structure in time and space. We then extended the model by adding a spatiotemporal interaction term, δ_{itk}, to deal with this issue. Thus,
$$\log(\eta_{itk}) = \mu_k + \sum_{m=1}^{M} X_{mitk}^T \beta_{mitk} + \alpha_{tk} + \gamma_{tk} + \theta_{ik} + \phi_{ik} + \delta_{itk} \tag{4-8}$$

The block $\delta_k = (\delta_{11k}, \ldots, \delta_{nTk})^T$ is also assumed to be Gaussian distributed with precision matrix $\kappa_{\delta_k} K_{\delta_k}$. Note that Eq. (4-8) will be reduced to Eq. (4-2) if all $\delta_{itk} = 0$. Hence δ_{itk} can capture the variations that cannot be explained by the main effect model. We assume the matrix K_{δ_k} as the Kronecker product of the structure matrices of those main effects (Clayton, 1996). This modeling mechanism can be considered as the Bayesian analogue of modeling interactions by tensor products in a spline regression framework (Stone et al., 1997). As shown in Eq. (4-8), there are four (2×2) possible combinations of interactions since each of the two temporal effects may have interactions with each of the two spatial effects. The symbolic representation of these four interactions is shown in Figure 4-4. Naturally, it indicates that different prior interrelationships should be assigned to different types of δ_{itk}. Following the article by Knorr‐Held (2000), the four types of δ_{itk} are separately discussed as follows, ordered by the degree of prior dependence.

(1) *Type uTuS*. In this type, the unstructured temporal effects γ_{tk} and the unstructured spatial effects ϕ_{ik} are expected to interact (as shown in the top-left subfigure in Fig. 4.4). Model with such type δ_{itk} can account for unobserved covariates for each pixel (i, t), but is unable to capture any structured effects in the time $\times$ space domain. Based on Clayton's rule (Clayton, 1996), $K_{\delta_k} = K_{\gamma_k} \otimes K_{\phi_k} = I \otimes I = I$, therefore, all interaction parameters δ_{itk} are a prior independent:

$$p(\delta_k | \kappa_{\delta_k}) \propto \exp(-\frac{\kappa_{\delta_k}}{2} \sum_{i=1}^{I} \sum_{t=1}^{T} (\delta_{itk})^2) \tag{4-9}$$
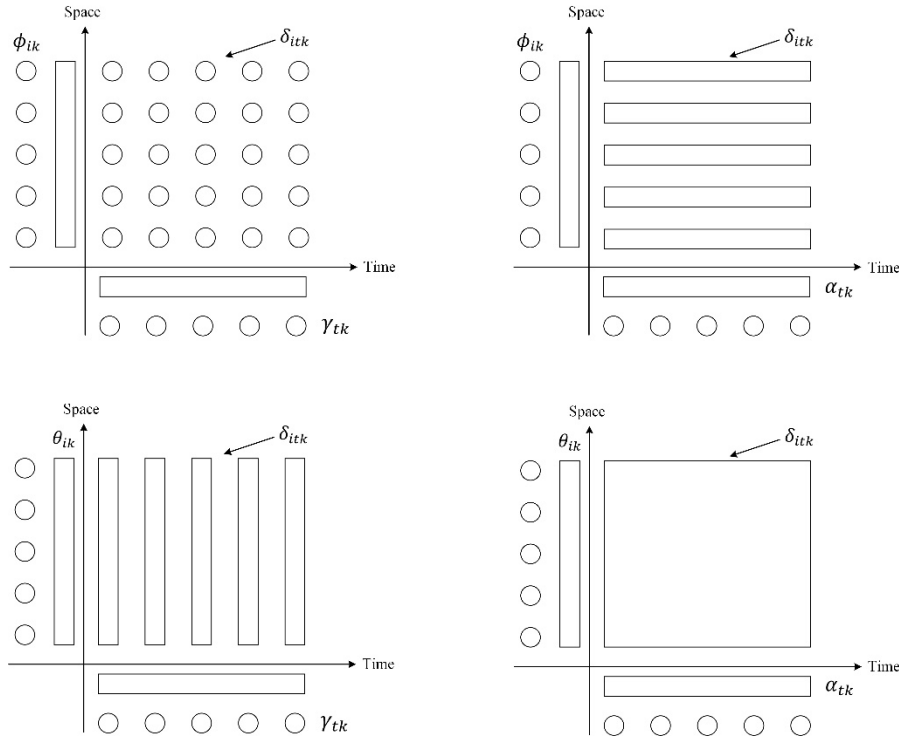

Figure 4-4 Symbolic Representation of Four Interactions (Rectangles Represent Prior Dependence, and Circles Represent Prior Independence)

(2) *Type sTuS*. In this type, the structured temporal effects α_{tk} and the unstructured spatial effects ϕ_{ik} are expected to interact (as shown in the top-right subfigure in Figure. 4-4). Model with this type δ_{itk}

can account for temporal trends that vary across counties, but has no structure in space. Note that $K_{\delta_k} = K_{\alpha_{tk}} \otimes K_{\phi_k} = K_{\alpha_{tk}} \otimes I = K_{\alpha_{tk}}$, then each $\delta_{ik} = (\delta_{i1k}, \dots, \delta_{iTk})^T$, $i = 1, \dots, n$, also follows a first order random walk, independently of all other counties. Thus, similar to Eq. (4-3), we have

$$p(\delta_k | \kappa_{\delta_k}) \propto \exp(-\frac{\kappa_{\delta_k}}{2} \sum_{i=1}^{I} \sum_{t=2}^{T} (\delta_{itk} - \delta_{i(t-1)k})^2) \tag{4-10}$$

(3) *Type uTsS*. In this type, the unstructured temporal effects γ_{tk} and the structured spatial effects θ_{ik} are expected to interact (as shown in the bottom-left subfigure in Figure. 4-4). Model with this type δ_{itk} can account for spatial trends that are different time point to time point, but has no temporal structure. Note that $K_{\delta_k} = K_{\gamma_{tk}} \otimes K_{\theta_{ik}} = I \otimes K_{\theta_{ik}} = K_{\theta_{ik}}$, therefore, each $\delta_{tk} = (\delta_{1tk}, \dots, \delta_{ntk})^T$, $t = 1, \dots, T$, also follows a non-stationary intrinsic autoregression. Thus, similar to Eq. (4-6), we have

$$p(\delta_k | \kappa_{\delta_k}) \propto \exp(-\frac{\kappa_{\delta_k}}{2} \sum_{t=1}^{T} \sum_{j \in N_i} (\delta_{itk} - \delta_{jtk})^2) \tag{4-11}$$

(4) *Type sTsS*. In this type, the two dependent and structured temporal and spatial effects, α_{tk} and θ_{ik}, are expected to interact (as shown in the bottom-right subfigure in Figure. 4-4). Model with δ_{itk} of this type can account both structured temporal and spatial effects. δ_{itk} is completely dependent over the time×space domain, and can no longer be factorized into independent blocks. The structure matrix K_{δ_k} then have characteristics of both random work and intrinsic autoregression approaches. The prior for δ_k can be written as

$$p(\delta_k | \kappa_{\delta_k}) \propto \exp(-\frac{\kappa_{\delta_k}}{2} \sum_{t=2}^{T} \sum_{j \in N_i} ((\delta_{itk} - \delta_{i(t-1)k}) - (\delta_{jtk} - \delta_{j(t-1)k}))^2) \tag{4-12}$$

with independent contrasts $((\delta_{itk} - \delta_{i(t-1)k}) - (\delta_{jtk} - \delta_{j(t-1)k}))$. The conditional distribution of δ_{itk}, which can be derived from $K_{\delta_k} = K_{\alpha_{tk}} \otimes K_{\theta_{ik}}$, has the mean

$$\mu_{itk} = \begin{cases} \delta_{i(t+1)k} + \frac{1}{\#N_i} \sum_{j \in N_i} \delta_{jtk} - \frac{1}{\#N_i} \sum_{j \in N_i} \delta_{j(t+1)k}, & \text{and } t = 1 \\ \delta_{i(t-1)k} + \frac{1}{\#N_i} \sum_{j \in N_i} \delta_{jtk} - \frac{1}{\#N_i} \sum_{j \in N_i} \delta_{j(t-1)k}, & \text{and } t = T \\ \frac{1}{2}(\delta_{i(t-1)k} + \delta_{i(t+1)k}) + \frac{1}{\#N_i} \sum_{j \in N_i} \delta_{jtk} - \frac{1}{2\#N_i} \sum_{j \in N_i} (\delta_{j(t-1)k} + \delta_{j(t+1)k}), & \text{and } t = 2, \dots, T-1 \end{cases} \tag{4-13}$$

and corresponding precision

$$\tau_{itk} = \begin{cases} \# N_i \kappa_{\delta_k}, & \text{and } t = 1 \text{ or } T \\ 2 \# N_i \kappa_{\delta_k}, & \text{and } t = 2, \dots, T-1 \end{cases} \tag{4-14}$$

Hence, the Type sTsS interaction prior is a Markov random field, where not only the first order temporal ($\delta_{i(t-1)k}$ and/or $\delta_{i(t+1)k}$) and spatial (δ_{jtk}) neighbours enter in the full conditional for δ_{itk}, but also the second order neighbours ($\delta_{j(t-1)k}$ and/or $\delta_{j(t+1)k}$), i.e., spatial neighbours of temporal neighbours or, equivalently, temporal neighbous of spatial neighbours. This prior "borrows strength" from its spatial neighbours as it assumes that the temporal trend in county i (in terms of first differences) is similar to the average trend in neighbouring counties (Cheng et al., 2018). Equivalently, one could also emphasize spatial trends here, as such a model "borrows strength" from neighbouring time points ($t-1$ and/or $t+1$), assuming the spatial pattern in year t is also assumed to be similar. It can be better seen from the conditional mean μ_{itk}, which satisfies both

$$\mu_{itk} - \bar{\delta}_{i \cdot k} = \bar{\delta}_{\cdot tk} - \bar{\delta}_{\cdot \cdot k} \tag{4-15}$$

and

$$\mu_{itk} - \bar{\delta}_{\cdot tk} = \bar{\delta}_{i \cdot k} - \bar{\delta}_{\cdot \cdot k} \tag{4-16}$$

where $\bar{\delta}_{i\cdot k}$ is the mean of the neighbors in time, $\bar{\delta}_{\cdot tk}$ is the mean of the neighbors in space, and $\bar{\delta}_{\cdot\cdot k}$ is the mean of the second order neighbors. Therefore, the temporal trend in county i is similar to the average trend in neighbouring counties. Equivalently, the spatial trend in year t is also assumed to be similar to the average trend in neighbouring time points. Therefore, such interaction type will be more suitable if temporal trends are different from county to county, but are more likely to be similar for adjacent counties.

The inclusion of the four types of spatiotemporal interaction terms allows more flexibility in the modeling framework as the temporal trend can deviate across different counties. This treatment allows the temporal trend of the empirical data to be more accurately represented, and meanwhile providing some smoothing in counties of extraordinarily high or low crash frequency. Finally, a comprehensive comparison of these four inseparable spatiotemporal interaction structures is presented in Table 4-2.

Table 4-2 Comparison of four spatiotemporal interaction structures

	Type uTuS	Type sTuS	Type uTsS	Type sTsS
Parameters interacting	γ_{tk} and ϕ_{ik}	α_{tk} and ϕ_{ik}	γ_{tk} and θ_{ik}	α_{tk} and θ_{ik}
Description	Interactions have no spatial or temporal patterns.	Interactions vary in time with trends differing by neighborhood.	Interactions have a trend in space. Nearby areas have similar differences from the overall trend in time.	Full spatiotemporal interactions. Nearby areas have similar but different trends.
Prior distribution used	Normally distributed	Random walk	Intrinsic autoregression	The Kronecker product of random walk in time and intrinsic autoregression in space

4.2.2. Prior Settings

In case of ambiguity, it should be mentioned that the following two forms of a priori hypothesis of a scalar c, which follows a highly dispersed diffuse Gaussian distribution, are equivalent:

$$c|\kappa_c \sim N(\mu, 1/\kappa_c) \tag{4-17}$$

$$p(c|\kappa_c) \propto \exp(-\frac{1}{2}\kappa_c c^2) \tag{4-18}$$

with μ as the prior mean and $1/\kappa_c$ arbitrarily small to reduce the prior's influence. With $\kappa_c \to 0$, the prior is diffuse. Taking additionally the posterior mean as a point estimate, the Bayes estimator and the least squares estimator become identical. For instance, one may often see the following form of an intrinsic conditional autoregressive model in previous studies (Lao et al., 2011):

$$\theta_{ik}|\theta_{jk(j\neq i)}, \kappa_{\theta_k} \sim N(\frac{1}{\#N_i}\sum_{j\in N_i}\theta_{jk}, \frac{1}{\#N_i\kappa_{\theta_k}}) \tag{4-19}$$

However, in essence, Eq. (4-19) is the same as Eq. (4-6), because it is just a rewritten form in terms of conditional distributions. Similarly, the other priors can also be rewritten in this way. Comparing Eq. (4-6) and Eq. (4-19), the interactions of the spatial neighbors in Eq. (4-6), i.e., $\theta_{ik} - \theta_{jk}$, are hidden in the conditional distribution form as only θ_{jk} is shown in Eq. (4-19). This situation also exists in other heterogeneity blocks (e.g., $\alpha_{tk} - \alpha_{(t-1)k}$, $\delta_{itk} - \delta_{jtk}$, etc.). Therefore, the authors believe that the

forms utilized in this study can more directly demonstrate the interactions between neighbors (i.e., time, spatial, and spatiotemporal neighbors), which may not be intuitively revealed by the conventional forms.

The five models we proposed are numbered here as (1) main effect only, (2) main effect with uTuS interaction prior, (3) main effect with sTuS interaction prior, (4) main effect with uTsS interaction prior, and (5) main effect with sTsS interaction prior. They are all built within the Bayesian hierarchical structure. For a fully Bayesian analysis, all the parameters are considered as unknown and estimated simultaneously together with unknown functions. The priors of parameters are set as follows:

$$\mu_k \sim U(-\infty, +\infty) \tag{4-20}$$

$$\beta_{.m} \sim N(0, 10000) \tag{4-21}$$

$$\sigma_{.m}^2 \sim \text{Inv} \sim \text{Gamma}(0.0001, 0.0001) \tag{4-22}$$

$$\kappa_{\alpha_k}, \kappa_{\gamma_k}, \kappa_{\theta_k}, \kappa_{\phi_k}, \kappa_{\delta_k} \sim \text{Gamma}(1, 0.01) \tag{4-23}$$

Therefore, the intercept item μ_k is assumed to follow a flat uniform distribution. For the randomly distributed coefficients $\beta_{mitk} \sim N(\beta_{.m}, \sigma_{.m}^2)$, we consider fairly non-informative normal and inverse gamma prior distributions for the parameters mean $\beta_{.m}$ and variation $\sigma_{.m}^2$. The Gamma priors in Eq. (4-23) are computationally convenient as the full conditional of κ will again be gamma distributed. For example, the precision $\kappa_{\alpha_k} \sim \text{Gamma}(a, b)$ has a full conditional $\kappa_{\alpha_k} \sim \text{Gamma}(a + \frac{1}{2}r(K_{\alpha k}), b + \frac{1}{2}\alpha_k' K_{\alpha k} \alpha_k)$, where $r(K_{\alpha k})$ is the rank of the matrix $K_{\alpha k}$. The selection of the shape and rate parameters of the gamma distributions are based on several tests considering model fit, sensitivity, as well as autocorrelations of parameters. In this study, highly dispersed Gamma hyperpriors are chosen for all blocks with values $a = 1$ and $b = 0.01$.

4.2.3. Model Performance and Comparison

Model fit is investigated using the posterior predictive check (Gelman et al., 1996). This self-consistency check evaluates whether the crash record data can reasonably be expected from the posterior predictive distribution. Replicated data simulated from the joint posterior predictive distribution is compared with the observations using the posterior predictive P values defined as follows:

$$P_{ek} = P(y_{ek}^{rep} \leq y_{ek} | y_k) \tag{4-24}$$

where y_k is the entire dataset (severity=k), y_{ek}^{rep} is the replicated value, and y_{ek} is the empirical value. Posterior predictive P-value near to zero or one indicates an ill-fitting model.

The deviance information criteria (DIC), which is widely used to evaluate hierarchical models, is also utilized in this study to take model complexity into account (Li et al., 2018b). The equation of DIC is defined as

$$\text{DIC} = D(\bar{\theta}) + 2pD = \bar{D} + pD \tag{4-25}$$

where $\bar{\theta}$ is the posterior mean of the parameters, $D(\bar{\theta})$ is the deviance at the posterior mean of the parameters, pD is the effective number of the model, and $\bar{D}$ is the mean of the sampled deviances from MCMC simulations. In general, differences in DIC more than 10 definitely rule out the model with the higher DIC, differences between 5 and 10 are considered substantial, and a difference of less than 5 indicates that the models are not statistically different (Spiegelhalter et al., 2014).

In addition, R_d^2 is also employed for model comparison and selection. R_d^2 is calculated as (Xu and Huang, 2015):

$$R_d^2 = 1 - \frac{\sum_{\forall i,t,k}(y_{itk}-\hat{\eta}_{itk})^2/\hat{\eta}_{itk}}{\sum_{\forall i,t,k}(y_{itk}-\bar{y})^2/\bar{y}} \tag{4-26}$$

where $\hat{\eta}_{itk}$ denotes the expected mean crash frequency obtained by the crash prediction models, and $\bar{y}$ is the average of crash frequency. The model with larger R_d^2 (towards the value of one) fits better to the data.

4.2.4. Random Effects Analysis

As a side effect of splitting the overall temporal effect into a structured block and an unstructured block, we are able to assess to some extent the amount of temporal dependency in the data by observing which one of the two effects exceeds. If the unstructured effect exceeds, the temporal dependency is smaller and vice versa. An approach comes straightforward, i.e., using the fraction of the smoothing precisions of the two effects as the criteria, thus

$$f_t = \frac{m(\kappa_{\alpha_k})}{m(\kappa_{\alpha_k})+m(\kappa_{\gamma_k})} \tag{4-27}$$

where f_t is the criteria measuring temporal dependency, and $m(\kappa_{\alpha_k})$, as well as $m(\kappa_{\gamma_k})$, are the mean values of the smoothing precisions of the structured and unstructured temporal effects, respectively. If f_t is close to one, indicating the structured temporal effect is smoother than the unstructured temporal effect, and unstructured effect exceeds, and the temporal dependency is unobvious. If f_t is close to zero, then the structured effect exceeds, and the temporal dependency is more significant.

Similarly, the spatial dependency criteria f_i is defined as

$$f_i = \frac{m(\kappa_{\theta_k})}{m(\kappa_{\theta_k})+m(\kappa_{\phi_k})} \tag{4-28}$$

where $m(\kappa_{\theta_k})$ and $m(\kappa_{\phi_k})$ are the mean values of the smoothing precisions of the structured and unstructured spatial effects, respectively. When f_i is close to one, the spatial dependency is unobvious. Otherwise, the spatial dependency is larger.

4.3. Model Estimation Results and Discussions

The main effect model and the other four models with different types of spatiotemporal interactions are all implemented in the R platform thorough the R2OpenBUGS package (Sturtz et al., 2010), which is a Bayesian analysis package using Markov chain Monte Carlo (MCMC) simulation to estimate posterior distributions of parameters (Sturtz et al., 2010). For each model, three simulation chains are run with 50,000 iterations for each chain, and the first 25,000 samples are discarded as burn-ins (Serhiyenko et al., 2016). The remaining 25,000 samples are retained to obtain the posterior distributions of parameters with a thinning interval of 5, and thus each chain records 5,000 samples. The experiments are separately conducted on a platform with an Intel Core i7-6700 CPU at 3.40 GHz processor and 16.0 GB RAM. Brooks-Gelman-Rubin statistic (Royle and Dorazio, 2006), the trace plots of estimated parameters, and the ratios of Monte Carlo deviations regarding the respective standard deviations of the estimations (should be less than 0.05) (Landau and Binder, 2014) are investigated and calculated to monitor model convergence. 95% Bayesian Credible Interval (BCI) of mean is provided to indicate the significance of the examined variables. Specifically, a variable is considered as significant if the 95% BCI of its estimated mean does not cover 0, and not significant if otherwise.

4.3.1.   Model Comparison Results

For the model specification, a Pearson correlation test is first performed to exclude the possibility of highly correlated variables. The Pearson product moment correlation coefficients of BD and INC, DVMT and POP, are equal to 0.837 and 0.782, respectively. The results indicate that there are high correlations within the two variable pairs, and the two variables in a pair should not be included together in the model. DIC and R_d^2 are also utilized to compare alternative models with different covariate subsets. The one that can produce a lower DIC value and a higher R_d^2 for the main effect model is considered superior and is retained in the model. Finally, based on these rules, BD, DVMT, MALE, UR, PAV, and LN are kept in the model, whereas INC and POP are eliminated.

Analyzing histograms of the posterior predictive P values of all the five models in Figure 4-5 can help us better assess the suitability of the models given the data. The vertical axis in each subfigure represents the count, and the horizontal axis represents the posterior predictive P values. 1-5 are the number of models, and a, b, and c represent the crash severities, i.e., minor injury crash, major injury crash, and fatal crash, respectively. A bell-shaped histogram indicates superior model fit (Meng, 1994). As shown in Figure 4-5, Model 1 are poorly fitted with pronounced u-shaped histograms in all three crash severities, and most of the P values are close to either 0 or 1. Comparing the subfigures of Model 1 with those of Models 2-5, the model fit is significantly improved when the spatiotemporal interaction term is included. The results indicate that the spatiotemporal interaction term can improve the model performance, and there exist some spatiotemporal effects in the crash-frequency data that cannot be fully revealed by the main effect model. As shown in Figure 4-5, one can easily figure out that Model 3 could provide the best fit overall since the subfigures 3a, 3b, and 3c all have lower values at the tails of the distribution and higher values at the center.

Table 4-3 presents the model comparison results using the penalized goodness of fit measures, i.e., DIC and R_d^2, for all the five models. Regarding the DIC values, all the models with the spatiotemporal interaction term δ_{itk} have lower DICs than the main effect model. The DIC differences between different models are all larger than 10, indicating that different models have significantly different goodness of fit. In particular, Model 3 has the lowest DIC, followed by Model 2. In terms of R_d^2, Model 3 has the highest value. Among all models with the spatiotemporal interaction term δ_{itk}, Model 4 is the worst-fit model (highest DIC and lowest R_d^2), and is not much better than Model 1. These results also suggest that the spatiotemporal variability in crash frequency could be better explained if the spatial and temporal effects in regression coefficients and the correlated interaction between them are simultaneously addressed. Besides, Model 3 performs best for our dataset, indicating that interaction between structured temporal effects and unstructured spatial effects can best capture the spatiotemporal heterogeneity that cannot be fully revealed by the main effect model. Thus, the Model 3 is preferred for this study and is selected as the final model for further analysis.
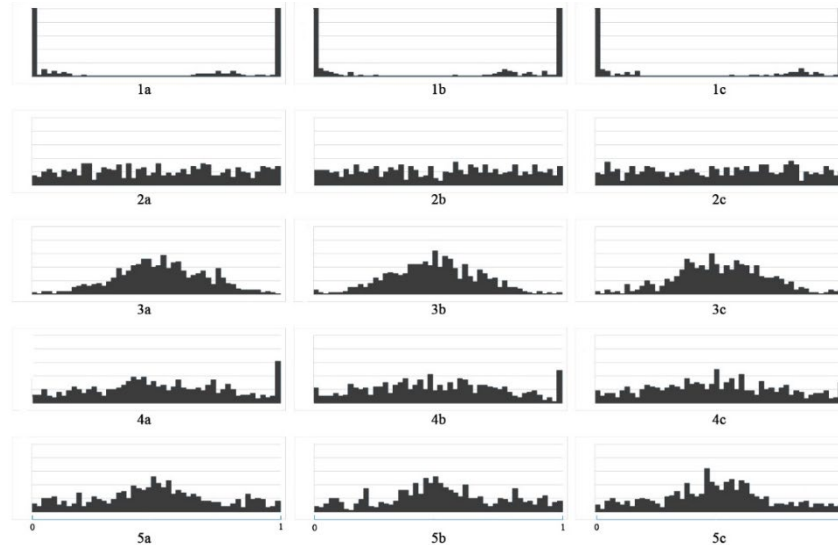
Figure 4-5 Histograms of Posterior Predictive P Values for All Models

Table 4-3 Model Performance Comparison for All Models

Model No.	Interactions	DIC	R_d^2
1	main effect	3233.65	0.64
2	main effect with uTuS interaction	3207.42	0.70
3	main effect with sTuS interaction	**3075.66**	**0.82**
4	main effect with uTsS interaction	3184.37	0.72
5	main effect with sTsS interaction	3135.21	0.78

4.3.2. Parameters Estimate Results

Table 4-4 summarizes the parameter estimates in Model 3. A variable is considered to be significant as long as one of the means or standard deviations of the parameters is significant. Once the standard deviation of a parameter is significant, the parameter is considered to be a random parameter. Otherwise, the variable is only considered to have a fixed effect across all observations. Since the means and the standard deviations of PAV and LN are all not significant for the three crash severities, they are excluded from the final model.

As shown in Table 4.4, the intercept term is significant for all three crash severities. DVMT is also statistically significant for all three crash severities because means and standard deviations of DVMT in different crash severities are all examined to be significant. The means of this variable are positive for all three crash severities, indicating that the counties with larger traffic volumes are more likely to have more alcohol/drug impaired driving crashes. This finding is consistent with previous studies (LaScala et al., 2000; Lee et al., 2015). They believe there are more alcohol/drug consumption places, e.g., groceries stores, bars, etc., at the crash site with higher DVMT. Besides, a higher traffic volume may also indicate that the crash site has more complex traffic conditions, regulations, control methods, etc., and requires drivers to have more precise control and faster response speeds, which are the capabilities impaired drivers lacking of. All of these reasons make DUI crashes easier to occur in places where DVMT is high. In

addition, the variable is found to be randomly distributed in all three crash severities, indicating there exists some unobserved heterogeneity associated with this variable. As figured out by Mannering et al. (2016a), due to unobserved time-varying environmental characteristics and unobserved variations in driver responses to traffic and these conditions, the effect of traffic volume on crash frequency is possible not to be constant along one roadway entity. Besides, road conditions (e.g., speed limit, the number of lanes, traffic control methods, etc.) of different roadways are very likely to be spatial instability even if they are in the same county, which may also induce unobserved heterogeneity to the data. Taking the random effects of this variable into consideration can better account for unobserved heterogeneity introduced by this variable, and we can be more confident to discern that the effect of traffic volume on crash frequency is non-linear (that is, the increase rate in the crash frequency caused by increases in traffic volume at higher congestion levels is different from that caused by increases in traffic volume at lower higher congestion levels).

The variable, MALE, denoting the proportion of males in a county, is observed to have a significant positive relationship with the likelihood of all three severities of DUI crashes. The finding is in line with numerous previous studies (Chen et al., 2016; Feng et al., 2016). According to the report of NHTSA, in 2016 there were 4 male alcohol-impaired drivers involved for every female alcohol-impaired driver involved (7,850 versus 1,883) (NHTSA, 2017). As evidenced by previous experiences and studies, males are much more likely to abuse alcohol and drugs than females in all age groups (Caetano et al., 2017). Some scholars also suggested that the ratio of male DUI drivers having personality traits, anti-sociality and risk-taking behaviors are higher than that of their female peers (Hingson and Winter, 2003). Therefore, it is not surprising that the increase in the proportion of males can increase the crash frequency. This variable is also found to be randomly distributed across the observations. This result indicates that there exist some variations across the population; for instance, body weight, amount of alcohol dehydrogenase, time spent drinking, driving behaviors, driving experiences and other factors that are generally unavailable to the analyst.

The variable, UR, denoting the unemployment rate in a county, is found to be randomly distributed across the observations and can significantly impact DUI crash frequency. Previous studies show that high unemployment rate may increase anxiety, psychological stress and depression in the population (Clark and Oswald, 1994; Dee, 2001; Wahlbeck and McDaid, 2012), as a result of income reductions and the subsequent loss of social status and relationships. In the field of psychology, the stress-response-dampening theory can explain the reasons of these crises-triggered consequences that could increase levels of alcohol consumption. The theory argues that individuals may consume more alcohol/drug during economic crises to reduce the intensity of their response to anxiety and stress, and some may even develop strong dependence on alcohol/drug (de Goeij et.al., 2015; Sher et al., 2007). In addition, a decrease in working hours will lead to individuals having more time for the activities that are often accompanied by alcohol consumption, e.g., sports activities, social events, and watching television (French et al., 2009). Consequently, it is not surprising that the higher unemployment rate could increase the alcohol/drug impaired-driving related crash frequency. In addition, as a random parameter for all three severities of crash, the effect of the unemployment rate in a county is likely to be a comprehensive function of a variety social and traffic conditions that are unknown to the analyst, thus causing heterogeneous effects across observations. For instance, when the unemployment rate is high, income reductions will result in tighter individual budget constraints. Thus, some drivers may choose to

drive less to save on gas, or may prefer to cut down alcohol or drug consumption to save money, both of which have negative impacts on the frequency of alcohol/drug impaired-driving related crash.

BD, indicating the percent of 25 years and older population with a bachelor's degree or higher, is the last variable that examined to have significant impacts on crash frequency. The coefficients of this variable are negative for all three severities of crashes, implying that less crashes are expected in the counties with a higher percentage of highly educated people. The reason may be that people with higher levels of education may have more knowledge about relevant regulations and laws on impaired driving. In addition, their low likelihood of alcohol/drug consumption or abuse may also contribute to these outcomes (Assari and Lankarani, 2016; Crum et al., 1993). It should also be noted that the variable was examined to have a strong correlation with the variable, INC, which is a variable indicating the average income level in a county. As also suggested by some economic theories, the individual prefers to spend less money on normal goods, including alcoholic beverages, when facing with an income reduction (Catalano, 1997). Thus, it is not surprising that this variable has a favorable impact on the frequency of DUI crashes. This variable is found to be randomly distributed for the observations, indicating some unobserved factors are likely to influence the impact of this variable.

Table 4-4 Estimated Parameters of Model 3 with Significant Covariates

Variables	Minor injury crash		Major injury crash		Fatal crash	
	Mean	95% BCI	Mean	95% BCI	Mean	95% BCI
Intercept	0.32	(0.20, 0.44)	1.77	(1.42, 2.03)	2.82	(2.55, 3.16)
Mean of Coefficients						
DVMT	0.54	(0.48, 0.62)	0.77	(0.68, 0.89)	1.33	(1.01, 1.57)
MALE	0.11	(0.08, 0.20)	0.12	(0.05, 0.19)	0.33	(0.23, 0.42)
UR	0.62	(0.47, 0.76)	0.44	(0.33, 0.56)	0.72	(0.63, 0.80)
BD	-0.13	(-0.21, 0.04)	-0.07	(-0.14, -0.01)	-0.10	(-0.18, -0.02)
Standard Deviation of Coefficients						
DVMT	0.12	(0.07, 0.20)	0.36	(0.18, 0.85)	0.04	(0.02, 0.06)
MALE	0.55	(0.49, 0.64)	0.22	(0.21, 0.24)	0.28	(0.22, 0.37)
UR	0.43	(0.35, 0.53)	0.34	(0.20, 0.55)	0.17	(0.15, 0.21)
BD	0.44	(0.42, 0.45)	0.10	(0.07, 0.15)	0.22	(0.16, 0.33)

Table 4-5 Estimated Spatiotemporal Random Effects of Model 3

Variables	Minor injury crash		Major injury crash		Fatal crash	
	Mean	95% BCI	Mean	95% BCI	Mean	95% BCI
Smoothing Precision						
κ_{γ_k}	0.34	(0.27, 0.44)	0.32	(0.27, 0.39)	0.35	(0.27, 0.44)
κ_{α_k}	0.79	(0.54, 1.11)	0.82	(0.57, 1.13)	0.81	(0.77, 0.88)
κ_{ϕ_k}	0.63	(0.40, 0.99)	0.48	(0.43, 0.55)	0.55	(0.42, 0.77)

κ_{θ_k}	0.85	(0.77, 0.94)	0.71	(0.65, 0.83)	0.68	(0.40, 0.97)
κ_{δ_k}	0.38	(0.28, 0.51)	0.94	(0.67, 1.30)	1.44	(1.30, 1.55)
Random Effects Dependency Criteria						
f_t	0.70		0.72		0.70	
f_i	0.57		0.60		0.55	

(a) Unstructured Effects   (b) Structured Effects   (c) All Effects
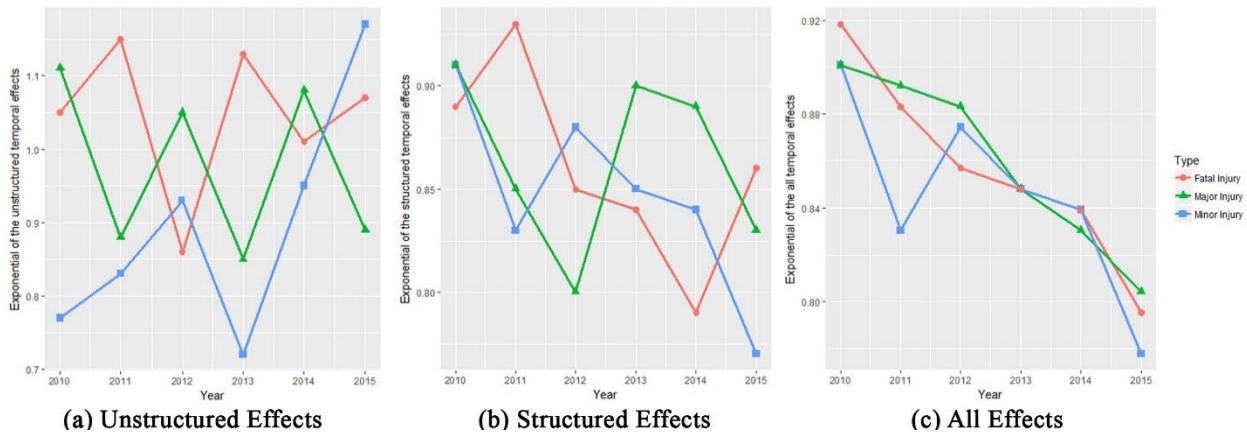
Figure 4-6 Exponential Posterior of Means of Temporal-related Effects

4.3.3. Random Effects Analysis

The estimated spatiotemporal random effects of Model 3 are presented in Table 4-5. Figures 4-6 and 4-7 illustrate the exponential posterior of means of all temporal-related effects and spatial-related effects, respectively. As shown in Table 4-5, unobserved heterogeneity in time exists both in individual years and between different years for all three crash severities. The mean of smoothing precisions for the unstructured temporal effects γ_{tk} in three crash severities are 0.34, 0.32, and 0.35, respectively. The estimated results indicate that the unstructured temporal effects are "seldom" smooth, i.e., the temporal instability effects within each year are significant. Figure 4-6 can better demonstrate this effect. Previous studies suggested that the exponential posterior of the mean of an effect can be considered as a relative risk (or odds ratio). If an exponential posterior of an effect is over one indicates that this effect has a positive impact on crash frequency, or decreases crash frequency otherwise (Aguero-Valverde and Jovanis, 2006; Bernardinelli et al., 1995). As shown in the subfigure (a) in Figure 4-6, in each crash severity, the exponential posteriors of means of the unstructured temporal effects $e^{\gamma_{tk}}$ are of significant differences in different years since the exponentials of means are distributed in a wide range. These results indicate the crash frequency in each year is not constant and may have month to month or seasonal fluctuations. The reason may be various. For instance, affected by climate factors, the per capita alcohol or drug consumption may vary in summer and winter, which may cause different crash frequency trends in different seasons in the same year. In addition, policy factors, such as intensive drunk driving inspections in a given month, may also have an impact on the distribution of crash frequency over time.

As shown in Table 4-5, the mean of smoothing precisions for the structured temporal effects α_{tk} in three crash severities are 0.79, 0.82, and 0.81, respectively. Therefore, the structured temporal effects

40

are much smoother than the unstructured effects for all three crash severities. As illustrated in the subfigure (b) in Figure 4-6, in each crash severity, the exponential posteriors of means of the structured temporal effects $e^{\alpha_{tk}}$ are mostly in (0.80, 0.90), indicating the temporal trends of crash frequency are decreasing over the years. These results are consistent with the temporal trends of empirically observed data. In addition, as illustrated in Table 4-5, the temporal random effects dependency criteria f_t for all three crash severities are equal to 0.70, 0.72, and 0.70, respectively. The results indicate the unstructured effect plays the main role and can explain more variability of the model in time.

Although both unstructured and structured temporal effects could capture some "pure" temporal heterogeneity in our data, they are not able to address the "mixed" temporal heterogeneity that has a relationship with spatial heterogeneity. The model comparison results suggest that there are some unobserved temporal variations that cannot be simply explained by the main effect model. Therefore, it is necessary to introduce the spatiotemporal interaction δ_{itk} for addressing this issue. Table 4-5 also provides estimated results of smoothing precisions for the spatiotemporal interaction for all three crash severities. The results show that the smoothing degrees of this interaction in different crash severities are significantly different (κ_{δ_k} equals to 0.38, 0.94, and 1.44, respectively), indicating the frequencies of different crash severities have different spatiotemporal trends. Combining all temporal-related effects together, the exponential posteriors of means of the overall temporal trend (Knorr‐Held, 2000), $e^{\alpha_{tk}+\gamma_{tk}+\delta_{itk}}$, are illustrated in the subfigure (c) in Figure 4-6. The exponential posteriors of means of overall temporal-related effects are all less than 1, indicating that the frequencies of all three crash severities are constantly decreasing in time.

Table 4-5 also presents estimation results for the mean of smoothing precisions of spatial related effects. The estimated results show that the unobserved heterogeneity in space exists both within individual counties and between counties. In each crash severity, the structured spatial effect θ_{ik} is smoother than the unstructured spatial effect ϕ_{ik} (κ_{ϕ_k} are equal to 0.63, 0.48, and 0.55, respectively; κ_{θ_k} are equal to 0.85, 0.71, and 0.68, respectively), indicating unstructured spatial effects can explain more "pure" spatial variation in the dataset. In addition, as illustrated in Table 4-5, the spatial effects dependency criteria f_i for all three crash severities are equal to 0.57, 0.60, and 0.55, respectively. The results also indicate the unstructured spatial effect plays the main role and can explain more variability of the model in space.

 Figure 4-7 presents the exponential posterior of means of unstructured spatial effects ($e^{\theta_{ik}}$), structured spatial effects ($e^{\phi_{ik}}$), and overall spatial-related effects ($e^{\theta_{ik}+\phi_{ik}+\delta_{itk}}$), respectively. As shown in subfigures (a), (b), and (c) in Figure 4-7, the unstructured spatial effects in each county are various among different crash severities. For the structured spatial effects illustrated in subfigures (d), (e), and (f) in Figure 4-7, these effects are much smoother than the unstructured spatial effects, and the counties that shared the same borders tend to have similar spatial trends. All the counties in Region 4 have positive structured spatial effects for all three crash severities, indicating these counties are associated with increasing trends in crash frequency. The counties in the neighboring regions of Region 4 (i.e., Region 2 and Region 3), "borrow" the spatial trends from the counties in Region 4, and also have positive structured spatial effects (but smaller than those of the counties in Region 4). Counties located in the regions far away from Region 4 are more likely to have negative structured spatial effects, indicating these areas are associated with decreasing trends in crash frequency. The results also imply that these farther counties are not able to "borrow" too much "strength" from Region 4. Comparing all

the spatial-related effects together, several counties are found to have significant increasing trends in crash frequency. The exponential posterior of means of overall spatial-related effects for all three crash severities in some counties, including Boise, Jerome, Kootenai, Nez Perce, Oneida, Shoshone, and Valley, are all larger than 1.5. The estimated results demonstrate that more specific countermeasures are needed in these counties to mitigate the potential increasing trends in crash frequency.
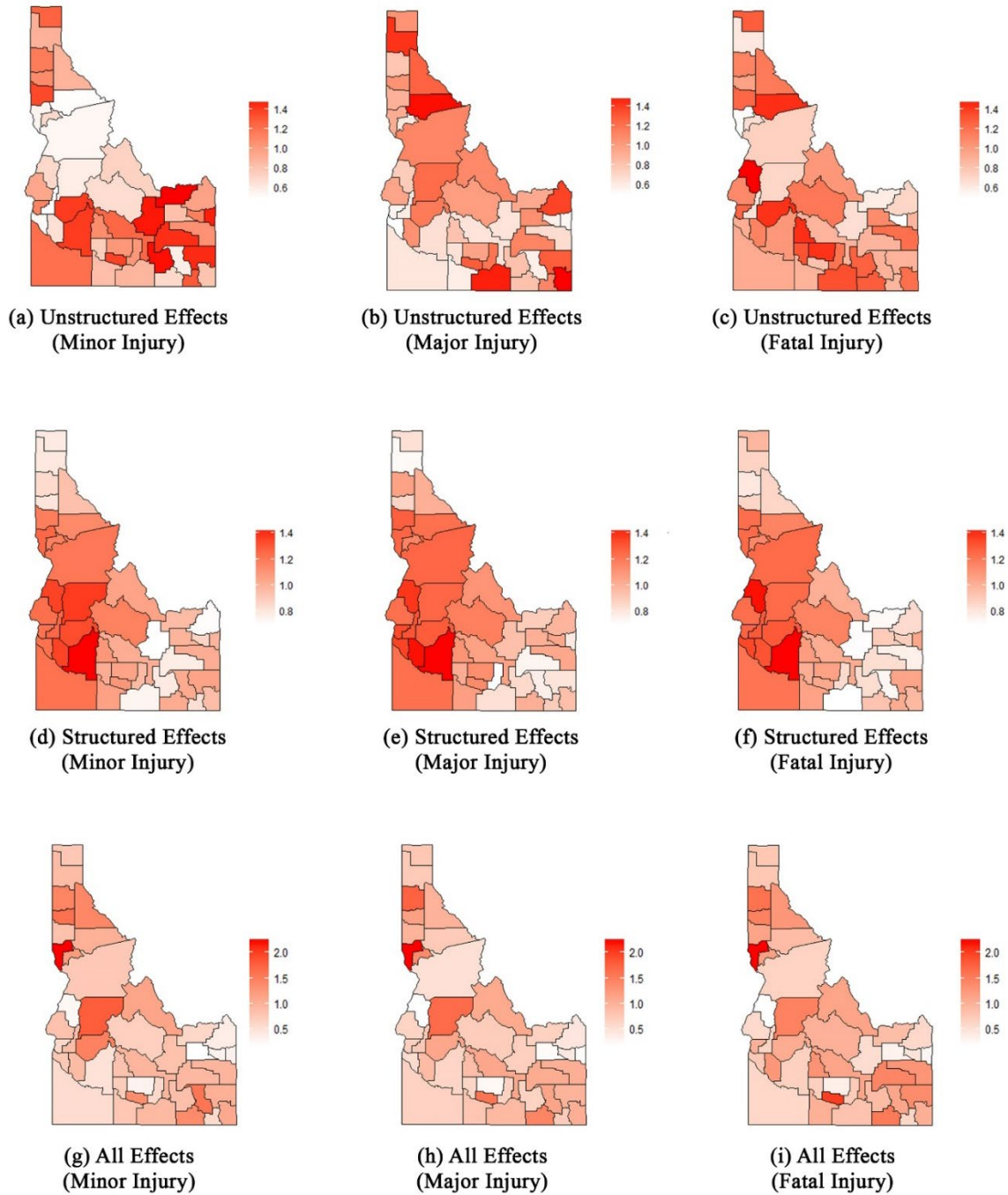

Figure 4-7 Exponential Posterior of Means of Spatial-related Effects

CHAPTER 5.   CONCLUSIONS AND RECOMMENDATIONS

5.1.   Conclusions

This report details the research activities undertaken to examine traffic crashes in RITI communities, which often result in severe injuries and significant losses. Unlike urban crashes, traffic incidents in RITI areas are more frequently associated with factors such as speeding, low usage of safety devices (e.g., seatbelts), adverse weather conditions, poor road maintenance, and inadequate lighting. Therefore, it is crucial to analyze the characteristics and attributes of traffic crashes in RITI communities using various data analysis methods, including statistical and data-driven approaches. However, traditional crash data analysis faces challenges due to unobserved heterogeneities and temporal instability.

In this study, a DNN structure, *i.e.*, the FCNN-R model, was proposed for driver injury severity analysis. The proposed FCNN-R model consists of a set of sub-NNs and a multi-layer CNN. More specifically, multiple sub-NNs are proposed for various categorical variables input; a random term is designed in the input layer to capture unobserved heterogeneities across individual crash records; the multi-layer CNN model captures the potential nonlinear relationship among impact factors and driver injury severity outcomes. The proposed model was fed with single-vehicle crash records acquired from the Washington State for the period of 2010 to 2016, including general crash information, driver information, vehicle information, and environmental information. The whole dataset is divided into three parts, i.e., the training, the validation, and the testing datasets. Different model layouts, i.e., different number of CNN layers and different techniques preventing from overfitting, are tested using the validation dataset. With the limited training data, more CNN layers result in the prematurity of the training algorithm applied in this study. Moreover, it is noted that the regularization and dropout techniques do improve the stability of the proposed model. However, they do not improve the predictive performance of the proposed model. The proposed FCNN-R model is compared with five typical approaches, i.e., the MNL, the MMNL, the NN, the CNN, and the FCNN model, using the test dataset. The comparison results indicate that the proposed model outperforms the other approaches in all the performance indices.

The comparison of the marginal effects between the proposed FCNN-R model and the MMNL model indicates that the DNN framework has the potential to capture the underlying relationship between various factors from vast data sources and driver injury severity outcomes. Once the model is well trained, the proposed FCNN-R can be used to not only predicting crash outcomes but also to estimate the effects of risk factors on injury severities. However, there exist several limitations of the proposed model. Firstly, the proposed model is only tested using single-vehicle crashes from the Washington States. For future research, the generalization and the transferability of the proposed mode shall be tested. Moreover, an improved model which allows absent variables would be pursued to improve the transferability of the proposed model for crash records with different variable sets. Secondly, the proposed model currently involves only crash records. We recommend including more information in the proposed model in a future study. Finally, advanced training algorithms for deeper models and more efficient model structures, such as the recurrent structures and the residual blocks, are of great interest and could be explored in the future.

In addition, traffic crashes are complex events because there are many observable or unobservable interactions between vehicles, traffic participants, road geometric characteristics, environmental conditions, etc., when the crashes occur. In view of these complex interactions, it seems impossible for

analysts to access all of the data that potentially determine the likelihood of crashes. This unobserved heterogeneity issue has been recognized and widely addressed by the random parameter's models in previous studies (Buddhavarapu, P., et al., 2016, Mannering, L., et al., 2016, Guo, Y., et al., 2019). Another issue that may also produce biased estimation and erroneous prediction is the temporal and spatial instability that brought by the conventionally aggregated crash-frequency data. Therefore, the two issues should not be ignored, and the models that can address both of them are more appropriate to analyze the crash-frequency data.

In this study, five hierarchical Bayesian random parameters models with different spatiotemporal interactions were developed to analyze the yearly county-level alcohol/drug impaired-driving related crash counts data of three different injury severities including minor injury, major injury, and fatal injury in Idaho from 2010 to 2015. Model comparison results show that the main effect model with the spatiotemporal interaction of structured temporal effects and unstructured spatial effects had the best model performance and was selected for further analysis. Daily vehicle miles traveled (DVMT), the proportion of male (MALE), unemployment rate (UR), and the percent of 25 years and older with a bachelor's degree or higher (BD) are found to have significant impacts on the frequencies of some crash severities. Pavement condition (PAV) and the number of lanes (LN) are not found significantly associated with crash frequencies for all the three crash severities and are thus removed from the final model. In addition, DVMT, MALE, UR, and BD are all found to be normally distributed for different crash severities, indicating there is some unobserved heterogeneity across the observations. The estimation results also provide conclusive evidence that the proposed model is able to capture the unobserved heterogeneity introduced by the explanatory variables.

Significant temporal and spatial heterogenous effects are also detected in all three crash severities. All three crash severities generally show significant descending temporal trends from 2010 to 2015. The examining results of all spatial-related effects also intuitively demonstrate the relative risks of all three crash severities in each county. The advantages of the proposed model are significant. Examining temporal- and spatial-related random effects can provide further insights rather than ambiguously regarding them as sources of overall unobserved heterogeneity or being included in noise terms. In addition, based on the estimated results, the analysts can easily figure out which county is associated an increasing trend of crash frequency, and can accordingly bring forward corresponding countermeasures for that county to reduce the likelihood of crashes. This approach allows us to gain a deeper understanding of the neighborhood variability, particularly when explanatory covariates are included, to examine whether the disparities in crash frequency are driven in large part by explanatory covariates or other ancillary considerations.

For further research, apart from the typically used random walk approach for structured temporal effects and Gaussian intrinsic autoregression approach for structured spatial effects, other temporal and spatial prior distributions can be attempted. Besides, smaller time×space domain, for instance, week×city domain, may produce more targeted and practical findings. In addition, only random effects are thought to be correlated in time and space, but regression coefficients may also be correlated in time and space. Thus, future researchers may want to consider spatiotemporal varying coefficient models.

5.2. Recommendations

To facilities future research, the following recommendations are made:

(1) Advanced training algorithms for deeper models and more efficient model structures, such as the recurrent structures and the residual blocks, are of great interest and could be explored in the future.

(2) Apart from the typically used random walk approach for structured temporal effects and Gaussian intrinsic autoregression approach for structured spatial effects, other temporal and spatial prior distributions can be attempted.

(3) Besides, smaller time×space domain, for instance, week×city domain, may produce more targeted and practical findings. In addition, only random effects are thought to be correlated in time and space, but regression coefficients may also be correlated in time and space. Thus, future researchers may want to consider spatiotemporal varying coefficient models.

REFERENCES

Abdelwahab, H., Abdel-Aty, M., 2002. Artificial neural networks and logit models for traffic safety analysis of toll plazas. Transportation Research Record. 1784, 115–125.

Abdelwahab, H., Abdel-Aty, M., 2001. Development of artificial neural network models to predict driver injury severity in traffic accidents at signalized intersections. Transportation Research Record. 1746, 6–13.

Abdel-Aty, M., Wang, X., 2006. Crash estimation at signalized intersections along corridors: analyzing spatial effect and identifying significant factors. Transportation Research Record: Journal of the Transportation Research Board 1953, 98–111.

Aguero-Valverde, J., Jovanis, P.P., 2006. Spatial analysis of fatal and injury crashes in Pennsylvania. Accident Analysis and Prevention 38(3), 618–625.

Al-Marshad, A., DeMers, G., & Kahn, C. (2013). National Highway Traffic Safety Administration (NHTSA) Notes. *Emerg Med*, *61*, 222.

Anastasopoulos, P.C., Mannering, F.L., 2009. A note on modeling vehicle accident frequencies with random-parameters count models. Accident Analysis and Prevention 41(1), 153–159.

Andrey, J., Yagar, S., 1993. A temporal analysis of rain-related crash risk. Accident Analysis and Prevention 25(4), 465–472.

Asbridge, M., Hayden, J.A., Cartwright, J.L., 2012. Acute cannabis consumption and motor vehicle collision risk: systematic review of observational studies and meta-analysis. Bmj 344, e536.

Assari, S., Lankarani, M.M., 2016. Education and alcohol consumption among older Americans; black–white differences. Frontiers in public health 4, 67.

Barua, S., El-Basyouny, K., Islam, M.T., 2016. Multivariate random parameters collision count data models with spatial heterogeneity. Analytic Methods in Accident Research 9, 1–15.

Behnood, A., Mannering, F.L., 2016. An empirical assessment of the effects of economic recessions on pedestrian-injury crashes using mixed and latent-class models. Analytic Methods in Accident Research 12, 1–17.

Bernardinelli, L., Clayton, D., Pascutto, C., Montomoli, C., Ghislandi, M., Songini, M., 1995. Bayesian analysis of space—time variation in disease risk. Statistics in medicine 14, 2433–2443.

Besag, J., 1991. Rejoinder. Annals of the institute of statistical mathematics 43(1), 45–59.

Besag, J., Green, P.J., 1993. Spatial statistics and Bayesian computation. Journal of the Royal Statistical Society. Series B (Methodological) 25–37.

Besag, J., Kooperberg, C., 1995. On conditional and intrinsic autoregressions. Biometrika 82(4), 733–746.

Bhat, C.R., Born, K., Sidharthan, R., Bhat, P.C., 2014. A count data model with endogenous covariates: formulation and application to roadway crash frequency at intersections. Analytic Methods in Accident Research 1, 53–71.

Blazquez, C.A., Celis, M.S., 2013. A spatial and temporal analysis of child pedestrian crashes in Santiago, Chile. Accident Analysis and Prevention 50, 304–311.

Buddhavarapu, P., Scott, J.G., Prozzi, J.A., 2016. Modeling unobserved heterogeneity using finite mixture random parameters for spatially correlated discrete count data. Transportation Research Part B, 91, 492–510.

Bao, J., Liu, P., Ukkusuri, S., 2019a. A spatiotemporal deep learning approach for citywide short-term crash risk prediction with multi-source data. Accident Analysis and Prevention. 122, 239–254.

Bao, J., Yu, H., Wu, J., 2019b. Short-term FFBS demand prediction with multi-source data in a hybrid deep learning framework. IET Intelligent Transport Systems, 13, 1340-1347.

Bengio, Y., Delalleau, O., 2011. On the expressive power of deep architectures, in: International Conference on Algorithmic Learning Theory. 18–36.

Blincoe, L., Miller, T., Zaloshnja, E., Lawrence, B., 2015. The economic and societal impact of motor vehicle crashes, 2010 (Revised). Washington DC.

Boureau, Y., Ponce, J., LeCun, Y., 2010. A theoretical analysis of feature pooling in vision algorithms, in: Proc. International Conference on Machine Learning.

Catalano, R., 1997. An emerging theory of the effect of economic contraction on alcohol abuse in the United States. Social Justice Research 10(2), 191-201.

Caetano, R., Schafer, J., Cunradi, C.B., 2017. Alcohol-related intimate partner violence among white, black, and Hispanic couples in the United States. Domestic Violence: The Five Big Questions.

Castro, M., Paleti, R., Bhat, C.R., 2012. A latent variable representation of count data models to accommodate spatial and temporal dependence: Application to predicting crash frequency at intersections. Transportation research part B 46(1), 253–272.

Chen, C., Zhang, G., Qian, Z., Tarefder, R.A., Tian, Z., 2016. Investigating driver injury severity patterns in rollover crashes using support vector machine models. Accident Analysis and Prevention 90, 128–139.

Chen, E., Tarko, A.P., 2014. Modeling safety of highway work zones with random parameters and random effects models. Analytic Methods in Accident Research 1, 86–95.

Cheng, W., Gill, G.S., Sakrani, T., Dasu, M., Zhou, J., 2017. Predicting motorcycle crash injury severity using weather data and alternative Bayesian multivariate crash frequency models. Accident Analysis and Prevention 108, 172–180.

Cheng, W., Gill, G.S., Zhang, Y., Cao, Z., 2018. Bayesian spatiotemporal crash frequency models with mixture components for space-time interactions. Accident Analysis and Prevention 112, 84–93.

Chiou, Y.-C., Fu, C., 2015. Modeling crash frequency and severity with spatiotemporal dependence. Analytic Methods in Accident Research 5, 43–58.

Clark, A.E., Oswald, A.J., 1994. Unhappiness and unemployment. The Economic Journal 104 (424), 648–659.

Clayton, D.G., 1996. Generalized linear mixed models. Markov chain Monte Carlo in practice 275–301.

Crum, R.M., Helzer, J.E., Anthony, J.C., 1993. Level of education and alcohol abuse and dependence in adulthood: a further inquiry. American Journal of Public Health 83(6), 830–837.

Chang, L., Wang, H., 2006. Analysis of traffic injury severity: An application of non-parametric classification tree techniques. Accident Analysis and Prevention. 38(5), 1019–1027.

Chen, C., Zhang, G., Huang, H., Wang, J., Tarefder, R., 2016. Examining driver injury severity outcomes in rural non-interstate roadway crashes using a hierarchical ordered logit model. Accident Analysis and Prevention. 96, 79–87.

Chen, C., Zhang, G., Ma, J., Wei, H., 2015. A multinomial logit model-Bayesian network hybrid approach for driver injury severity analyses in rear-end crashes. Accident Analysis and Prevention. 80, 76–88.

Delen, D., Sharda, R., Bessonov, M., 2006. Identifying significant predictors of injury severity in traffic accidents using a series of artificial neural networks. Accident Analysis and Prevention. 38(3), 434–444.

Dimopoulos, Y., Bourret, P., Lek, S., 1995. Use of some sensitivity criteria for choosing networks with good generalization ability. Neural Processing Letters. 2, 1–4.

Dee, T.S., 2001. Alcohol abuse and economic conditions: evidence from repeated cross-sections of individual-level data. Health economics 10(3), 257–270.

Dong, N., Huang, H., Lee, J., Gao, M., Abdel-Aty, M., 2016. Macroscopic hotspots identification: A Bayesian spatio-temporal interaction approach. Accident Analysis and Prevention 92, 256–264.

El-Basyouny, K., Sayed, T., 2009a. Collision prediction models using multivariate Poisson-lognormal regression. Accident Analysis and Prevention 41(4), 820–828.

El-Basyouny, K., Sayed, T., 2009b. Urban arterial accident prediction models with spatial effects. Transportation Research Record: Journal of the Transportation Research Board 2102, 27–33.

Fountas, G., Anastasopoulos, P., Abdel-Aty, M., 2018. Analysis of accident injury-severities using a correlated random parameters ordered probit approach with time variant covariates. Analytic Methods in Accident Research. 18, 57–68.

Feng, S., Li, Z., Ci, Y., Zhang, G., 2016. Risk factors affecting fatal bus accident severity: Their impact on different types of bus drivers. Accident Analysis and Prevention 86, 29–39.

French, M. T., Popovici, I., Maclean, J. C., 2009. Do alcohol consumers exercise more? Findings from a national survey. American Journal of Health Promotion, 24(1), 2-10.

Gelman, A., Meng, X.-L., Stern, H., 1996. Posterior predictive assessment of model fitness via realized discrepancies. Statistica sinica, 733–760.

Guo, F., Wang, X., Abdel-Aty, M.A., 2010. Modeling signalized intersection safety with corridor-level spatial correlations. Accident Analysis and Prevention 42(1), 84–92.

Garson, G., 1991. Interpreting Neural Network Connection Weights. AI Expert. 6(4), 47–51.

Guidotti, R., Monreale, A., Ruggieri, S., Turini, F., Giannotti, F., Pedreschi, D., 2018. A survey of methods for explaining black box models. ACM Computing Surveys. 51(5), 93.

Guo, Y., Li, Z., Liu, P., Wu, Y., 2019. Modeling correlation and heterogeneity in crash rates by collision types using full bayesian random parameters multivariate Tobit model. Accident Analysis and Prevention. 128, 164–174.

Highway Safety Annual Report. (2014). Hawaii State Department of Transportation. https://hidot.hawaii.gov/highways/files/2013/01/2014-Annual-Report.pdf

Hingson, R., Winter, M., 2003. Epidemiology and consequences of drinking and driving. Alcohol Research and Health 27(1), 63–78.

Huang, H., Abdel-Aty, M., Darwiche, A., 2010. County-level crash risk analysis in Florida: Bayesian spatial

modeling. Transportation Research Record: Journal of the Transportation Research Board 2148, 27–37.

Huang, H., Chin, H., Haque, M., 2009. Empirical evaluation of alternative approaches in identifying crash hot spots: naive ranking, empirical Bayes, and full Bayes methods. Transportation Research Record: Journal of the Transportation Research Board 2103, 32–41.

Huang, H., Zhou, H., Wang, J., Chang, F., Ma, M., 2017. A multivariate spatial model of crash frequency by transportation modes for urban intersections. Analytic Methods in Accident Research 14, 10–21.

Hailesilassie, T., 2016. Rule extraction algorithm for deep neural networks: A review. International Journal of Computer Science and Information Security. 14(7), 376-381.

He, K., Zhang, X., Ren, S., Sun, J., 2015. Delving deep into rectifiers: Surpassing human-level performance on imagenet classification, in: Proceedings of the IEEE International Conference on Computer Vision. 1026–1034.

Hu, W., Donnell, E., 2010. Median barrier crash severity: Some new insights. Accident Analysis and Prevention. 42(6), 1697–1704.

Idaho Transportation Department, 2015. Idaho Traffic Crashes 2015.

Islam, S., Mannering, F., 2006. Driver aging and its effect on male and female single-vehicle accident injuries: Some additional evidence. Journal of Safety Research. 37(3), 267–276.

Jalayer, M., Shabanpour, R., Pour-Rouholamin, M., Golshani, N., Zhou, H., 2018. Wrong-way driving crashes: A random-parameters ordered probit analysis of injury severity. Accident Analysis and Prevention 117, 128–135.

Ke, J., Zheng, H., Yang, H., Chen, X., 2017. Short-term forecasting of passenger demand under on-demand ride services: A spatio-temporal deep learning approach. Transportation Research Part C. 85, 591–608.

Keramati, A., Lu, P., Iranitalab, A., Pan, D., Huang, Y., 2020. A crash severity analysis at highway-rail grade crossings: The random survival forest method. Accident Analysis and Prevention. 144, 105683.

Khattak, A., 2001. Injury severity in multivehicle rear-end crashes. Transportation Research Record. 1746, 59–68.

Knorr-Held, L., 2000. Bayesian modelling of inseparable space-time variation in disease risk. Statistics in medicine 19(17-18), 2555–2567.

Lee, J., Abdel-Aty, M., Choi, K., Huang, H., 2015. Multi-level hot zone identification for pedestrian safety. Accident Analysis and Prevention 76, 64–73.

Li, Y.C., Sze, N.N., Wong, S.C., 2013. Spatial–temporal analysis of drink-driving patterns in Hong Kong. Accident Analysis and Prevention 59, 415–424.

Li, Z., Chen, C., Wu, Q., Zhang, G., Liu, C., Prevedouros, P.D., Ma, D.T., 2018a. Exploring driver injury severity patterns and causes in low visibility related single-vehicle crashes using a finite mixture random parameters model. Analytic Methods in Accident Research 20, 1–14.

Li, Z., Chen, C., Ci, Y., Zhang, G., Wu, Q., Liu, C., Qian, Z. (Sean), 2018b. Examining driver injury severity in intersection-related crashes using cluster analysis and hierarchical Bayesian models. Accident

Analysis and Prevention 120, 139–151.

Liu, C., Sharma, A., 2018. Using the multivariate spatio-temporal Bayesian model to analyze traffic crashes by severity. Analytic Methods in Accident Research 17, 14–31.

Liu, C., Sharma, A., 2017. Exploring spatio-temporal effects in traffic crash trend analysis. Analytic Methods in Accident Research 16, 104–116.

Liu, C., Zhao, M., Li, W., Sharma, A., 2018. Multivariate random parameters zero-inflated negative binomial regression for analyzing urban midblock crashes. Analytic Methods in Accident Research 17, 32–46.

Lee, C., Abdel-Aty, M., 2008. Presence of passengers: does it increase or reduce driver's crash potential? Accident Analysis and Prevention. 40(5), 1703–1712.

Lee, J., Mannering, F., 2002. Impact of roadside features on the frequency and severity of run-off-roadway accidents: An empirical analysis. Accident Analysis and Prevention. 34(2), 149–161.

Li, X., Lord, D., Zhang, Y., Xie, Y., 2008. Predicting motor vehicle crashes using Support Vector Machine models. Accident Analysis and Prevention. 40(4), 1611–1618.

Li, Z., Chen, C., Ci, Y., Zhang, G., Wu, Q., Liu, C., Sean, Z., 2018. Examining driver injury severity in intersection-related crashes using cluster analysis and hierarchical Bayesian models. Accident Analysis and Prevention. 120, 139–151.

Li, Z., Ci, Y., Chen, C., Zhang, G., Wu, Q., Sean, Z., Prevedouros, P., Ma, D., 2019. Investigation of driver injury severities in rural single-vehicle crashes under rain conditions using mixed logit and latent class models. Accident Analysis and Prevention. 124, 219–229.

Lord, D., Mannering, F., 2010. The statistical analysis of crash-frequency data: A review and assessment of methodological alternatives. Transportation Research Part A. 44(5), 291–305.

Lv, Y., Duan, Y., Kang, W., Li, Z., Wang, F., 2014. Traffic flow prediction with big data: a deep learning approach. IEEE Transactions on Intelligent Transportation Systems. 16(2), 865–873.

Ma, X., Chen, S., Chen, F., 2017. Multivariate space-time modeling of crash frequencies by injury severity levels. Analytic Methods in Accident Research 15, 29–40.

Mannering, F., 2018. Temporal instability and the analysis of highway accident data. Analytic Methods in Accident Research 17, 1–13.

Mannering, F.L., Shankar, V., Bhat, C.R., 2016. Unobserved heterogeneity and the statistical analysis of highway accident data. Analytic Methods in Accident Research 11, 1–16.

Ma, X., Tao, Z., Wang, Yinhai, Yu, H., Wang, Yunpeng, 2015a. Long short-term memory neural network for traffic speed prediction using remote microwave sensor data. Transportation Research Part C. 54, 187–197.

Ma, X., Yu, H., Wang, Yunpeng, Wang, Yinhai, 2015b. Large-scale Transportation Network Congestion Evolution Prediction Using Deep Learning Theory. PLoS One. 10, 1–17.

Mannering, F., 2018. Temporal instability and the analysis of highway accident data. Analytic Methods in Accident Research. 17, 1–13.

Mannering, F., Bhat, C., Shankar, V., Abdel-Aty, M., 2020. Big data, traditional data and the tradeoffs between prediction and causality in highway-safety analysis. Analytic Methods in Accident Research. 25, 100113.

Meng, X.-L., 1994. Posterior predictive p-values. The Annals of Statistics 22(3), 1142–1160.

Milton, J.C., Shankar, V.N., Mannering, F.L., 2008. Highway accident severities and the mixed logit model: an exploratory empirical analysis. Accident Analysis and Prevention 40(1), 260–266.

Musenge, E., Chirwa, T.F., Kahn, K., Vounatsou, P., 2013. Bayesian analysis of zero inflated spatiotemporal HIV/TB child mortality data through the INLA and SPDE approaches: Applied to data observed between 1992 and 2010 in rural North East South Africa. International journal of applied earth observation and geoinformation 22, 86–98.

Nguyen, H., Kieu, L., Wen, T., Cai, C., 2018. Deep learning methods in transportation domain: a review. IET Intelligent Transport Systems. 12(9), 998–1004.

NHTSA, 2017. 2016 Fatal Motor Vehicle Crashes: Overview. Traffic Safety Facts: Research Note (DOT HS 812456) 1–9.

O'donnell, C., Connor, D., 1996. Predicting the severity of motor vehicle accident injuries using models of ordered multiple choice. Accident Analysis and Prevention. 28(6), 739–753.

Olden, J., Jackson, D., 2002. Illuminating the "black box": a randomization approach for understanding variable contributions in artificial neural networks. Ecological Modelling. 154(1-2), 135–150.

Ouyang, Y., Shankar, V., Yamamoto, T., 2002. Modeling the simultaneity in injury causation in multivehicle collisions. Transportation Research Record. 1784, 143–152.

Quddus, M.A., 2008. Modelling area-wide count outcomes with spatial correlation and heterogeneity: an analysis of London crash data. Accident Analysis and Prevention 40(4), 1486–1497.

Royle, J.A., Dorazio, R.M., 2006. Hierarchical models of animal abundance and occurrence. Journal of Agricultural, Biological, and Environmental Statistics 11(3), 249–263.

Serhiyenko, V., Mamun, S.A., Ivan, J.N., Ravishanker, N., 2016. Fast Bayesian inference for modeling multivariate crash counts. Analytic Methods in Accident Research 9, 44–53.

Sher, K. J., Bartholow, B. D., Peuser, K., Erickson, D. J., Wood, M. D., 2007. Stress-response-dampening effects of alcohol: Attention as a mediator and moderator. Journal of Abnormal Psychology, 116(2), 362.

Spiegelhalter, D.J., Best, N.G., Carlin, B.P., Linde, A., 2014. The deviance information criterion: 12 years on. Journal of the Royal Statistical Society: Series B (Statistical Methodology) 76, 485–493.

Stone, C.J., Hansen, M.H., Kooperberg, C., Truong, Y.K., 1997. Polynomial splines and their tensor products in extended linear modeling: 1994 Wald memorial lecture. The Annals of Statistics 25(4), 1371–1470.

Sturtz, S., Ligges, U., Gelman, A., 2010. R2OpenBUGS: a package for running OpenBUGS from R. URL http://cran. rproject. org/web/packages/R2OpenBUGS/vignettes/R2OpenBUGS. pdf.

Sameen, M., Pradhan, B., 2017. Severity prediction of traffic accidents with recurrent neural networks. Applied Science. 7(6), 476.

Sameen, M., Pradhan, B., Shafri, H., Hamid, H., 2017. Applications of deep learning in severity prediction of traffic accidents, in: Global Civil Engineering Conference. 793–808.

Savolainen, P., Mannering, F., Lord, D., Quddus, M., 2011. The statistical analysis of highway crash-injury severities: A review and assessment of methodological alternatives. Accident Analysis and Prevention. 43(5), 1666–1676.

Scherer, D., Müller, A., Behnke, S., 2010. Evaluation of pooling operations in convolutional architectures for object recognition, in: International Conference on Artificial Neural Networks. 92–101.

Schmidhuber, J., 2015. Deep learning in neural networks: An overview. Neural Networks 61, 85–117.

Shankar, V., Mannering, F., Barfield, W., 1996. Statistical analysis of accident severity on rural freeways. Accident Analysis and Prevention. 28(3), 391–401.

Shibata, A., Fukuda, K., 1994. Risk factors of fatality in motor vehicle traffic accidents. Accident Analysis and Prevention. 26(3), 391–397.

Srivastava, N., Hinton, G., Krizhevsky, A., Sutskever, I., Salakhutdinov, R., 2014. Dropout: a simple way to prevent neural networks from overfitting. Journal of Machine Learning Research. 15(56), 1929–1958.

Wang, X., Abdel-Aty, M., 2006. Temporal and spatial analyses of rear-end crashes at signalized intersections. Accident Analysis and Prevention 38(6), 1137–1150.

Wang, X., Abdel-Aty, M., Brady, P., 2006. Crash estimation at signalized intersections: significant factors and temporal effect. Transportation Research Record: Journal of the Transportation Research Board 1953(1), 10–20.

Wahlbeck, Kristian, and David McDaid., 2012. Actions to alleviate the mental health impact of the economic crisis. World psychiatry 11(3), 139-145.

Williams, D., Haworth, J., Blangiardo, M., Cheng, T., 2018. A spatiotemporal bayesian hierarchical approach to investigating patterns of confidence in the police at the neighborhood level. Geographical Analysis.

Wu, Q., Chen, F., Zhang, G., Liu, X.C., Wang, H., Bogus, S.M., 2014. Mixed logit model-based driver injury severity investigations in single-and multi-vehicle crashes on rural two-lane highways. Accident Analysis and Prevention 72, 105–115.

Wang, X., Abdel-Aty, M., 2008. Analysis of left-turn crash injury severity by conflicting pattern using partial proportional odds models. Accident Analysis and Prevention. 40(5), 1674–1682.

Wang, Y., Zhang, D., Liu, Y., Dai, B., Lee, L., 2019. Enhancing transportation systems via deep learning: A survey. Transportation Research Part C. 99, 144-163.

Wu, Q., Chen, F., Zhang, G., Liu, X., Wang, H., Bogus, S., 2014. Mixed logit model-based driver injury severity investigations in single-and multi-vehicle crashes on rural two-lane highways. Accident Analysis and Prevention. 72, 105–115.

Wu, Q., Zhang, G., Ci, Y., Wu, L., Tarefder, R., Alcantara, A., 2016a. Exploratory multinomial logit model--based driver injury severity analyses for teenage and adult drivers in intersection-related crashes. Traffic Injury Prevention. 17(4), 413–422.

Wu, Q., Zhang, G., Zhu, X., Cathy, X., Tarefder, R., 2016b. Analysis of driver injury severity in single-vehicle crashes on rural and urban roadways. Accident Analysis and Prevention. 94, 35–45.

Xie, Y., Lord, D., Zhang, Y., 2007. Predicting motor vehicle collisions using Bayesian neural network models: An empirical analysis. Accident Analysis and Prevention. 39(5), 922–933.

Xie, Y., Zhang, Y., Liang, F., 2009. Crash injury severity analysis using Bayesian ordered probit models. Journal of Transportation Engineering. 135(1), 18–25.

Xie, Y., Zhao, K., Huynh, N., 2012. Analysis of driver injury severity in rural single-vehicle crashes. Accident Analysis and Prevention. 47, 36–44.

Xie, K., Wang, X., Ozbay, K., Yang, H., 2014. Crash frequency modeling for signalized intersections in a high-density urban road network. Analytic Methods in Accident Research 2, 39–51.

Xu, P., Huang, H., 2015. Modeling crash spatial heterogeneity: random parameter versus geographically weighting. Accident Analysis and Prevention 75, 16–25.

Xiong, Y., Tobias, J., Mannering, F., 2014. The analysis of vehicle crash injury-severity data: A Markov switching approach with road-segment heterogeneity. Transportation Research Part B. 67, 109–128.

Ye, F., Lord, D., 2014. Comparing three commonly used crash severity models on sample size requirements: multinomial logit, ordered probit and mixed logit models. Analytic Methods in Accident Research. 1, 72–85.

Yu, H., Chen, X., Li, Z., Zhang, G., Liu, P., Yang, J., Yang, Y., 2020a. Taxi-based mobility demand formulation and prediction using conditional generative adversarial network-driven learning approaches. IEEE Transactions on Intelligent Transportation Systems. 20(10), 3888–3899.

Yu, H., Yuan, R., Li, Z., Zhang, G., Ma, D., 2020b. Identifying heterogeneous factors for driver injury severity variations in snow-related rural single-vehicle crashes. Accident Analysis and Prevention. 144, 105587.

Yu, M., Ma, C., Shen, J., 2021. Temporal stability of driver injury severity in single-vehicle roadway departure crashes: A random thresholds random parameters hierarchical ordered probit approach. Analytic Methods in Accident Research. 29, 100144.

Yu, M., Zheng, C., Ma, C., Shen, J., 2020. The temporal stability of factors affecting driver injury severity in run-off-road crashes: A random parameters ordered probit model with heterogeneity in the means approach. Accident Analysis and Prevention. 144, 105677.

Yu, R., Zheng, Y., Qin, Y., Abdel-Aty, M., 2020. Crash injury severity analyses with multilevel thresholds of change modelling approach for at-fault out-of-state drivers. Journal of Transportation Safety and Security. 12, 1164-1181.

Zeng, Q., Gu, W., Zhang, X., Wen, H., Lee, J., Hao, W., 2019. Analyzing freeway crash severity using a Bayesian spatial generalized ordered logit model with conditional autoregressive priors. Accident Analysis and Prevention. 127, 87–95.

Zeng, Q., Huang, H., 2014. Bayesian spatial joint modeling of traffic crashes on an urban road network. Accident Analysis and Prevention 67, 105–112.

Zeng, Q., Hao, W., Lee, J., Chen, F., 2020. Investigating the impacts of real-time weather conditions on freeway crash severity: A bayesian spatial analysis. International Journal of Environmental Research and Public Health. 17(8), 2768.

Zeng, Q., Huang, H., 2014. A stable and optimized neural network model for crash injury severity prediction. Accident Analysis and Prevention. 73, 351–358.

Zeng, Q., Huang, H., Pei, X., Wong, S., 2016a. Modeling nonlinear relationship between crash frequency by severity and contributing factors by neural networks. Analytic Methods in Accident Research. 10, 12–25.

Zeng, Q., Huang, H., Pei, X., Wong, S., Gao, M., 2016b. Rule extraction from an optimized neural network for traffic crash frequency modeling. Accident Analysis and Prevention. 97, 87–95.

Zheng, M., Li, T., Zhu, R., Chen, J., Ma, Z., Tang, M., Cui, Z., Wang, Z., 2019. Traffic Accident's Severity Prediction: A Deep-Learning Approach-Based CNN Network. IEEE Access 7, 39897–39910.